ALL ASPECTS OF FIBROSIS

International Workshop
BERLIN, GERMANY

October 23, 2025

5 CME CREDITS

5 credit hours (CME) have been awarded by the European Union of Medical Specialists (UEMS).

PREFACE

All Aspects of Fibrosis

The concepts on the pathophysiology of organ fibrosis in general and in particular in gastrointestinal (GI) diseases are rapidly evolving. Until recently fibrosis was regarded as a consequence of long standing inflammation followed by scar formation and collagen deposition. Once established, fibrosis appeared to be an irreversible process that could be barely influenced. Therefore, the main goal in GI diseases associated with fibrosis such as viral induced liver fibrosis or Crohn's disease was to control inflammation in order to prevent fibrosis development. Many of these previous assumptions, however, need to be revisited.

Recent data indicate that liver fibrosis is (at least) partially reversible. In addition first drugs to treat fibrosis have been approved. The clinical pre-requisites to study treatment of fibrosis have been established. Due to these swiftly increasing insights into fibrogenesis, it is timely to focus on "all aspects of fibrosis" to learn from other fibrotic diseases outside of GI, discuss their mechanisms and experience with diagnosis and treatments, and discuss on how to apply those to GI related fibrosis. We are fortunate to have recruited excellent speakers and experts that will provide us with the latest insights into fibrosis pathophysiology, diagnosis and treatment options.

We are thrilled to welcome you to Berlin and are sure that this international Falk Foundation Workshop will foster future research in the field and bring you insights that are already highly valuable for clinical practice.

Florian Rieder

Gerhard Rogler

ALL ASPECTS OF FIBROSIS

October 23, 2025

Scientific Organization:
Florian Rieder, Cleveland (United States)
Gerhard Rogler, Zurich (Switzerland)

Congress Venue:
JW Marriott Hotel Berlin
Stauffenbergstr. 26
10785 Berlin
Germany

For admission to scientific events your name badge should be clearly visible.

Accompanying persons are not permitted during the conference at any time.

Start of Registration:
Wednesday, October 22, 2025
16:00-20:00 h
at the congress office

Start of ePoster Session:
Thursday, October 23, 2025
08:30 h

Thursday, October 23, 2025

09:00 Welcome
Florian Rieder, Cleveland; Gerhard Rogler, Zurich

SESSION I

Keynote

Chairs: *Florian Rieder, Cleveland; Gerhard Rogler, Zurich*

09:10 The future of therapies to alter wound healing: From discovery to medicines
Michael Longaker, Stanford

SESSION II

Mechanisms of fibrosis

Chairs: *Valerie Horsley, New Haven; Sonya MacParland, Toronto*

09:40 Mechanobiology and fibroblast function
Boris Hinz, Toronto

09:55 Fibrometabolism: The new frontier?
Rachel Chambers, London

10:10 Fibroblast with macrophage crosstalk in tissue repair and fibrosis
Valerie Horsley, New Haven

10:25 **Coffee break with ePoster session**

SESSION III

Fibroblast heterogeneity: One size does not fit all

Chairs: *Suzanne Devkota, Los Angeles; Boris Hinz, Toronto*

11:00	Fibroblast lineages in lung inflammation and fibrosis *Dean Sheppard, San Francisco*
11:20	Fibroblast driven mechanisms in liver fibrosis *Neil Henderson, Edinburgh*
11:40	Fibroblast driven mechanisms in intestinal fibrosis *Florian Rieder, Cleveland*
12:00	Fibroblast heterogeneity in skin fibrosis *Joerg Distler, Erlangen*
12:20	**Lunch break with ePoster session**

SESSION IV

Intestinal fibrosis

Chairs: *Giovanni Latella, L'Aquila; Azuzena Salas, Barcelona*

14:00	**Presentation of Poster Awards** *Florian Rieder, Cleveland; Gerhard Rogler, Zurich*
14:20	Adipose tissue fibrosis *Suzanne Devkota, Los Angeles*
14:40	Mechanisms of intestinal fibrosis *Gerhard Rogler, Zurich*
15:00	Cytokines and cytokine networks in stricturing Crohn's disease *Markus Neurath, Erlangen*
15:20	**Coffee break with ePoster session**

Thursday, October 23, 2025

SESSION V	
Measuring and treating fibrosis: Successes and Failures	
Chairs:	*Massimo Pinzani, Palermo; Anja Poulsen, Copenhagen*
16:00	Serum markers of fibrosis *Morten A. Karsdal, Copenhagen*
16:20	Imaging of fibrosis of the bowel *Jordi Rimola, Barcelona*
16:40	The road to antifibrotics in idiopathic pulmonary fibrosis *Gisli Jenkins, London*
17:00	Clinical trial endpoints in liver fibrosis *Frank Tacke, Berlin*
17:20	Closing remarks

LIST OF SPEAKERS, MODERATORS AND SCIENTIFIC ORGANIZERS

Prof. Dr. Rachel Chambers
University College London
Centre for Inflammation and
Tissue Repair,
5 University Street,
London, WC1E 6JJ,
United Kingdom

Suzanne Devkota, PhD
Cedars-Sinai Medical Center
Davis Building, D-4007
8700 Beverly Blvd
Los Angeles, CA 90048
United States

Prof. Dr. Joerg Distler
Kinder- und Jugendabteilung für
Psychische Gesundheit
Universitätsklinikum Erlangen
Schwabachanlage 6 und 10
91054 Erlangen
Germany

Prof. Neil Henderson, MD PhD
Centre of Inflammation Research
Institute for Regeneration and Repair
The University of Edinburgh
5 Little France Dr
EH16 4UU, Edinburgh
United Kingdom

Prof. Boris Hinz, PhD
St. Michael's Hospital
Laboratory of Tissue Repair and
Regeneration
Keenan Research Centre for Biomedical
Science
Unity Health
209 Victoria Street
ON M5B 1T8, Toronto
Canada

Prof. Valerie Horsley, PhD
Yale School of Medicine
409 Prospect St
CT 06511, New Haven
United States

Prof. Gisli Jenkins
Margaret Turner Warwick Centre for
Fibrosing Lung Disease
National Heart and Lung Institute
Imperial College London
Guy Scadding Building
Cale Street
London, SW3 6LY
United Kingdom

Prof. Morten A. Karsdal, mMBA PhD
Nordic Bioscience A/S,
Herlev Hovedgade 205
2730 Herlev
Denmark

Prof. Giovanni Latella
Gastroenterology Unit
Department of Life, Health and Environmental Sciences
University of L'Aquila
Piazza S. Tommasi, 1-Coppito
67100 L'Aquila
Italy

Prof. Dr. Michael Longaker
Stanford Medicine
Hagey Building
257 Campus Dr Room GK106
MC 5148
Stanford CA 94305
United States

Dr. Sonya MacParland
Department of Laboratory Medicine & Pathobiology
University of Toronto
Office 2-308 101 College Street
Toronto, M5G 1L7
Canada

Prof. Dr. Markus Neurath
Deutsches Zentrum Immuntherapie
Medizin 1
Uniklinik Erlangen
Ulmenweg 18
91054 Erlangen
Germany

Prof. Massimo Pinzani
ISMETT
Via E. Tricomi 5
90127 Palermo
Italy

Ass. Prof. Anja Poulsen
Department of Digestive Diseases Transplantation and General Surgery
Section for IBD
Rigshospitalet
Inge Lehmanns Vej 5
2100 Copenhagen
Denmark

Dr. Florian Rieder, M.D.
Dept. of Gastroenterology, Hepatology and Nutrition
Digestive Diseases and Surgery Institute
The Cleveland Clinic Foundation
9500 Euclid Avenue
Cleveland, OH 44195
United States

Dr. Jordi Rimola
IBD unit, Radiology department
Hospital Clínic de Barcelona
CIBER-EHD, IDIBAPS
C/ Villarroel, 170
08036 Barcelona
Spain

Prof. Dr. Dr. Gerhard Rogler
Klinik für Gastroenterologie und Hepatologie
UniversitätsSpital Zürich
Rämistr. 100
8091 Zürich
Switzerland

Prof. Dr. Azucena Salas
IDIBAPS, CIBER-EHD
Rosselló 149
Barcelona 08036
Spain

Dr. Dean Sheppard
University of California, San Francisco
PO BOX 589001, Room 252R
San Francisco, CA 94158-9001
United States

Prof. Dr. Frank Tacke
Medizinische Klinik mit Schwerpunkt
Hepatologie und Gastroenterologie
Charité - Universitätsmedizin Berlin
Augustenburger Platz 1
13353 Berlin
Germany

REGISTRATION

You can register for the event via our homepage:
www.falkfoundation.org
Registration is only possible online.

CONGRESS FEES

Scientific Program of International Workshop	EUR 150
Students (copy of student ID required)	EUR 75

The congress fees include:
– Pre-Opening and Welcome on Wednesday, October 22, 2025
– Refreshments during coffee breaks
– Lunch on Thursday, October 23, 2025
– A copy of the final program

CONGRESS OFFICE AND REGISTRATION

Opening Hours:

Wednesday, October 22, 2025	16:00 - 20:00 h
Thursday, October 23, 2025	8:00 – 20:00 h

The Falk Foundation will take pictures during the meeting. Additionally, parts of the meeting might be recorded. By participating all attendees consent and agree with the recording and the photo shoots.

GENERAL INFORMATION

The event “All Aspects of Fibrosis, International Workshop Berlin, Germany” is organized by the Falk Foundation e.V.

The Falk Foundation covers the travel expenses for speakers as well as their hotel and registration costs. The Falk Foundation e.V. also bears the costs for catering, room rental and technical equipment. The organizer is associated with Dr. Falk Pharma GmbH.

ARRIVAL

JW Marriott Hotel Berlin
Stauffenbergstr. 26
10785 Berlin
Germany

By plane
The Berlin Brandenburg Airport (BER) is about 26.5 km away from the hotel and well connected with trains departing from Terminal 1-2 every hour. You can also take a taxi which takes about 30 minutes time.

By train
Berlin Central Station (U-Bahn, S-Bahn, regional trains, ICE train)
Station Potsdamer Platz (U-Bahn, S-Bahn, regional trains)
From Station Potsdamer Platz: Head west on Potsdamer Platz/B1.
Turning right toward Sigismundstrasse. Slight right onto Sigismundstrasse. Turn left onto Stauffenbergstrasse. Destination will be on the left.

By car
On-Site Parking
Hourly: €3.00
Daily: €25.00

CONFLICTS OF INTEREST

The members of the scientific committe declare the following potential conflicts of interest:

Florian Rieder: Consultant or Advisor: Údiso, Adnovate, Agomab, Allergan, AbbVie, Arena, Astra Zeneca, Bausch & Lomb, Boehringer-Ingelheim, Celgene/BMS, Celltrion, CDISC, Celsius, Cowen, 89Bio, Eugit, Ferring, Galapagos, Galmed, Genentech, Gilead, Gossamer, Granite, Guidepoint, Helmsley, Horizon Therapeutics, Image Analysis Limited, Index Pharma, Landos, Jannsen, Koutif, Mestag, Metacrine, Mirum, Mobius, Mopac, Morphic, Myka Labs, Organovo, Origo, Palisade, Pfizer, Pliant, Prometheus Biosciences, Receptos, RedX, Roche, Samsung, Sanofi, Surmodics, Surrozen, Takeda, Techlab, Teva, Theravance, Thetis, Tr1x Bio, UCB, Ysios

Gerhard Rogler has consulted to Abbvie, Arena, Augurix, BMS, Boehringer, Catypso, Celgene, Eli Lilly, Falk, Ferring, Fisher, Genentech; Gilead, h1Dex, Janssen, MSD, Novartis, Pfizer, Phadia, Pierre Fabre, Roche, UCB, Tillots, Vifor, Vital Solutions and Zeller; Gerhard Rogler has received speaker's honoraria from Abbvie, Astra Zeneca, BMS, Celgene, EH Lilly, Falk, Janssen, MSD, Pfizer, Phadia, Pierre Fabre, Takeda, Tillots, UCB, Vifor and Zeller; Gerhard Rogler has received educational grants and research grants from Abbvie, Ardeypharm, Augurix, calypso, Falk, Flamentera, MSD, Novartis, Pfizer, Roche, Takeda, Tillots, UCB and Zeller. Gerhard Rogler is cofounder and head of the scientific advisory board of PharmaBiome.

POSTER ABSTRACTS

1. Multimodal imaging of collagen structure, immune cell distribution, and gene expression in fibrotic tissues
   M. Aaa Hegazi, M. Chiriva-Internati, F. Pasqualini, F. Grizzi (Rozzano, IT; Houston, US)
2. The angiotensin II antagonist, losartan, modulates intestinal fibrosis in experimental Crohn's disease-like ileitis
   S. Artone, J. Williams, K. Akbulut, K. Vidmar, H. Wargo, T. Parigi, D. Pietropaoli, G. Latella, C. De Salvo, T. Pizarro, S. De Santis (Cleveland, US; L'Aquila, IT)
3. Correlations between liver fibrosis severity and risk factors in metabolic dysfunction-associated fatty liver disease (MAFLD)
   C. Atodiresei (Iasi, RO)
4. Role of CCL5 in the pathology of hepatitis delta infection
   B. Bartosch, E. Batbold, O. Khomich, J. Molle, A. Roca Suarez, X. Grand, A. Ivanov, F. Zoulim (Lyon, FR; Moscow, RU)
5. Primary ileocecal lymphoma presented by chronic diarrhea and treated with drugs
   M. Basaranoglu, M. Bilgic (Istanbul, TR)
6. Fibroscan can diagnose NASH associated cirrhosis before decompasion hepatic
   N. Bozkurt, N. Bozkurt, M. Basaranoglu (Istanbul, TR)
7. Decompensated liver disease: Quality improvement project
   L. Carneiro, A. Lodhi, R. Nongrum (Sheffield, GB)
8. High dimensional analysis of murine lung bleomycin time course reveals key factors contributing to inflammation, fibrosis, and resolution of injury
   S. Christensen, I. Lee, W. Zang, J. Wang, K. Gerlovin, F. Schlerman (Cambridge, US; Berlin, DE)
9. Effect of a multi-strain probiotic formulation on the reduction of intestinal fibrosis through the modulation of TGF-β1 signalling pathways: In vitro study
   A. Ciafarone, F. Augello, V. Ciummo, S. Altamura, S. Artone, F. Lombardi, P. Palumbo, B. Cinque, G. Latella (L'Aquila, Chieti, IT)
10. Circulating bone marrow-derived stem cells and serum stem cell factor levels in chronic hepatitis C: Relation to hepatic fibrosis and activation of hepatic stellate cells
    H. El Aggan, N.M. Farahat, B.M. El Sabaa, A.S. Elyamany, R.M. Aboy Esa (Alexandria, EG)
11. Increased macrophage activation marker CD163 is associated with significant liver fibrosis and metabolic derangements in hepatitis C virus-infected patients with metabolic dysfunction-associated steatotic liver disease (MASLD)
    H. El Aggan, S. Mahmoud, N. El Deeb, A. Elyamany, D. Hosny (Alexandria, EG)
12. Fibrotic processes in Fuchs endothelial corneal dystrophy
    M. Fros, N. Demiralay, M. Simon, Z. Xinlei, B. Bjoern, O. Margarete (Cologne, DE)
13. Comprehensive analysis of mesenchymal cells involvement in mouse liver fibrosis
    W. Gao, H. El Mourabit, T. Jaffredo, S. Lemoinne, C. Housset, N. Chignard, A. Cadoret (Paris, FR)

14. Role of budesonide in improvement of the fibrosis in patients with primary biliary cirrhosis after incomplete response to UDCA monotherapy
A. Genunche-Dumitrescu, C. Neagoe, C. Badea, R. Surugiu, C. Deliu, A. Badea (Craiova, Bals, Bucharest, RO)

15. Identifying microbial drivers of fibrostenotic stricturing Crohn's disease
R. Giri, A. Amiss, S. Li, J. Begun (Brisbane, AU)

16. Comparing the use of liver fibrosis scores in MASLD/MASH and comorbidities
I. Hryhorchuk, L. Sydorchuk, R. Sydorchuk, B. Lytvyn, A. Sydorchuk, I. Sydorchuk, M. Yarynych, I. Sydorchuk (Chernivtsi, UA; Neu-Ulm, Siegen, DE)

17. Metabolic dysfunction-associated steatotic liver disease is a risk factor for the development of liver fibrosis in patients with multiple myeloma undergoing chemotherapy
G. Maslova, E. Stadnik (Poltava, UA)

18. Evaluation of liver fibrosis in patients with NAFLD and cutaneous psoriasis compared to patients with NAFLD
C. Neagoe, S. Ianosi, V. Neagoe, A. Genunche-Dumitrescu, M. Popescu, A. Amzolini (Craiova, RO)

19. Differential risk of dysplasia in small-duct versus large-duct primary sclerosing cholangitis in IBD patients: A retrospective study
N. Nishad, S. Subramanian, S. Janarthanan, M. Thoufeeq (Sheffield, Cambridge, GB)

20. Smart phone application to exclude varices in compensated cirrhosis with liver transaminases, liver and splenic stiffness using transient elastography
N. Nishad, M. Niriella, A. De Silva, G. Hewathanthri (Sheffield, GB; Ragama, Colombo, LK)

21. Plectin loss disrupts mechanotransduction and attenuates hepatic stellate cell activation
S. Ojha (Prague, CZ)

22. Hepatocellular carcinoma surveillance at Bradford Royal Infirmary – A single centre AUDIT of surveillance outcomes
M. Salman (Bradford, GB)

23. Fibrosis and steatosis assessment in chronic hepatitis B: Correlation with viral replication
G. Sarbu, A. Jucan, C. Mihai, I. Mihai, C. Atodiresei, A. Lungu, O. Nedelciuc, M. Dranga, C. Cijevschi Prelipcrean, C. Mihai (Iasi, RO)

24. Stage-specific drivers of clinical progression in advanced chronic liver disease
G. Semmler, B. Simbrunner, M. Bofill Roig, E. Meyer, L. Balcar, M. Jachs, L. Hartl, B. Hofer, G. Kramer, P. Thoene, C. Sebesta, N. Dominik, R. Marculescu, P. Quehenberger, B. Scheiner, P. Schwabl, A. Staettermayer, M. Trauner, T. Reiberger, M. Mandorfer (Vienna, AT; Barcelona, ES)

25. Ischemic heart disease is associated with liver fibrosis in patients with metabolic dysfunction-associated steatotic liver disease
I. Skrypnyk, G. Maslova, I. Pilat, V. Ostrovskyi (Poltava, UA)

26. Transient elastography and non-invasive fibrosis scores in infantile lysosomal acid lipase deficiency (Wolman disease)
M. Slae, E. Shteyer (Jerusalem, IL)

27. Intestinal fibrosis in IBD: Linkage with opportunistic infections, mesenteric vessels endothelial dysfunction and colonic resistance may have possible genetic background
A. Sydorchuk, L. Sydorchuk, B. Lytvyn, R. Sydorchuk, M. Yarynych, I. Sydorchuk, I. Sydorchuk, P. Kyfiak (Neu-Ulm, Siegen, DE; Chernivtsi, UA)

28. Genetically determined linkage of leptin, fibrosis, and hepatic dysfunction in MASLD
L. Sydorchuk, B. Lytvyn, R. Sydorchuk, A. Sydorchuk, M. Yarynych, I. Sydorchuk, I. Hryhorchuk, I. Sydorchuk (Chernivtsi, UA; Neu-Ulm, Siegen, DE)

29. Complex interplay of hepatic fibrosis, inflammation and immune response in experimental fast-food and methionine-choline-deficient diets
R. Sydorchuk, A. Sydorchuk, B. Lytvyn, L. Sydorchuk, M. Yarynych, I. Sydorchuk, I. Sydorchuk, P. Kyfiak, I. Plehutsa (Chernivtsi, Storozhynets, UA; Neu-Ulm, Siegen, DE)

30. Discriminative value, associations and mediating effects of inflammatory markers for MASLD, at-risk MASH and increased liver stiffness in 11,072 U.S. individuals
L. Van Kleef, I. Ayada, J. Pustjens, F. Tacke, W. Brouwer (Rotterdam, NL, Berlin, DE)

31. Evaluating the diagnostic accuracy of non-invasive fibrosis scores against Metavir staging in chronic liver disease
D. Zaric, A. Milic, D. Vrinic-Kalem, D. Zlatkovic, M. Gacinovic, P. Svorcan (Belgrade, RS)

32. In vivo CRISPR/Cas9 screens identify cell death inducing DFFA-like effector B as a therapeutic target of MASH
X. Zhong, A. Bogomolova, Q. Peng, V. Hamann, S. Hook, Q. Yuan, H. Bantel, H. Wedemeyer, M. Ott, A. Balakrishnan, A. Sharma (Hannover, DE)

FULL CONTENT OF POSTER ABSTRACTS

Poster Numbers 1 – 32

1. Multimodal imaging of collagen structure, immune cell distribution, and gene expression in fibrotic tissues

Mohamed Aaa Hegazi (Rozzano, IT), Maurizio Chiriva-Internati (Houston, US), Fabio Pasqualini (Rozzano, IT), Fabio Grizzi (Rozzano, IT)

Introduction: Fibrosis, a feature of many chronic diseases, results from a dysregulated tissue repair response and shares mechanisms with wound healing. In liver disease, it is driven by complex factors including inflammation, cytokines, hepatocyte apoptosis, oxidative stress, microbiome changes, and environmental influences. While traditionally assessed via biopsy and semi-quantitative scoring systems, newer imaging and computer-aided methods offer more precise evaluation. Still, non-invasive tools have limitations, and biopsy remains necessary when critical diagnostic or research data are needed. We present a quantitative approach combining multiplexed fluorescence IHC (mIF) to profile immune cells, polarized light imaging to assess collagen type and alignment, and RNAscope® (ACD Technologies, Italy) to detect mRNA transcripts. This integrated method enables simultaneous analysis of immune activity, extracellular matrix (ECM) structure, and gene expression within a single tissue section.

Methods: Three-micrometer FFPE biopsy and surgical liver tissue sections were deparaffinized and stained using TSA-based Opal 9 multiplex immunofluorescence (Opal 7-Color, Akoya Biosciences). Antibodies (mouse anti-human CD68, mouse anti-human CD45, mouse anti-human CD3, Dako) were paired with Opal fluorophores based on expected expression levels. DAPI was used for nuclear counterstaining. Whole-slide images were acquired at 20× magnification using a Zeiss Axioscan Z1. Slides were then stained with Picrosirius Red and counterstained with Hematoxylin. Brightfield and polarized light imaging (20×, Zeiss Axioscan Z1) were used to evaluate ECM coverage and collagen type, respectively. A computer-aided image analysis system was used to quantify a set of morphological features from mIF, brightfield, and polarized light images. Consecutive tissue sections were also processed with RNAscope to detect mRNA transcripts alongside mIF, brightfield, and polarized light imaging, enabling an integrated analysis of immune activity, ECM structure, and gene expression. We defined a new quantitative parameter, the Collagen Maturity Index (CMI). Using polarized light images of the same histological sections, analysis was performed in RGB space. Pixels were selected based on specific red (R min–R max) and green (G min–G max) intensity ranges to create separate red and green masks. For each mask, the mean intensity (μ) was calculated as: $\mu = (1/N) \sum x_i$. The CMI was then defined as the ratio of mean green to mean red intensity: CMI = μ green/μ red

Results: The tested methodology is resulted helpful without generation of tissue damage and artifacts. mIF revealed distinct spatial distributions of immune cell

populations, including CD68 macrophages, CD45 leukocytes, and CD3 T cells, within fibrotic liver tissue. Polarized light imaging differentiated collagen fiber types (collagen type I and III) and demonstrated altered fiber alignment associated with fibrosis severity. RNAscope analysis enabled the detection of specific mRNA transcripts within immune cell-rich and fibrotic regions, highlighting localized gene expression changes. The integration of these modalities through computer-aided image analysis provided a comprehensive, quantitative assessment of liver fibrosis, linking immune cell infiltration, ECM remodeling, and gene expression within the same tissue context.

Discussion/Conclusion: mIF is a powerful technique that enables in situ visualization of complex immune phenotypes within the tumor immune microenvironment by leveraging distinct spectrometric signatures. When integrated with brightfield and polarized light imaging for assessing collagen-rich ECM, alongside histochemical, mIF, and mRNA-based analyses, this multiscale approach offers a detailed perspective on the dynamic processes driving fibrosis. Incorporating concepts such as scale, geometry, fiber alignment, spatial organization, and non-linear interactions with immune and stromal cell populations, this strategy underscores the need for multidisciplinary expertise. Beyond enhancing our understanding of fibrotic progression, this integrative methodology also holds promise for advancing the development and clinical translation of antifibrotic therapies. Given that fibrosis can affect multiple organs, including the heart, lungs, liver, kidneys, skin, and bone marrow, this approach has broad applicability across general and systemic pathology.

2. The angiotensin II antagonist, losartan, modulates intestinal fibrosis in experimental Crohn's disease-like ileitis

Serena Artone (Cleveland, US), Joseph Williams (Cleveland, US), Kenan Akbulut (Cleveland, US), Kaylynn Vidmar (Cleveland, US), Hannah Wargo (Cleveland, US), Tommaso Parigi (Cleveland, US), Davide Pietropaoli (L'Aquila, IT), Giovanni Latella (L'Aquila, IT), Carlo De Salvo (Cleveland, US), Theresa Pizarro (Cleveland, US), Stefania De Santis (Cleveland, US)

Introduction: Fibrotic complications affect over half of Crohn's disease (CD) patients, particularly in the ileum, and current treatment options remain limited, with non-invasive therapies representing an unmet need for fibrostenosing CD. The renin-angiotensin system (RAS) contributes to intestinal inflammation and fibrosis, and angiotensin II receptor 1 (AT1) blockers (ARBs), such as Losartan (Los), may aid in mitigating these processes. Although RAS modulation has been explored in inflammatory bowel disease (IBD), previous studies have utilized animal models that are typically acute, self-resolving, and restricted to the colon. Here, we aimed to assess the anti-fibrotic potential of Los using the SAMP1/YitFc (SAMP) mouse strain, which develops chronic ileitis and ileal fibrosis similar to CD.

Methods: AT1 expression was assessed using bulk RNA-Seq data (GSE193677) and immunohistochemistry (IHC) on CD patient biopsies. CCD18-Co cells were

treated with angiotensin II (Ang II) ± Los, and profibrotic transcripts measured. RAS-associated genes were evaluated in SAMP and control AKR ilea at 4 and 30 weeks. SAMP mice were treated with Los or placebo for 10 weeks; tissues were analyzed for inflammation, fibrosis, and fibrosis-associated gene expression.

Results: AT1 was reduced in IBD tissues by bulk RNA analysis, but elevated in fibrotic regions by IHC, localizing primarily to the muscularis propria and submucosa. In vitro, Ang II stimulation of CCD18-Co cells increased profibrotic gene expression, which was reversed by Los. In SAMP mice, early-stage disease showed RAS activation, with upregulation of Angiotensinogen (Agt) and Renin (Ren), and downregulation of angiotensin-converting enzyme (Ace). In advanced disease, Agt, Ace, and Agtr1 were downregulated, while Ren and Ace2 were upregulated. In vivo, losartan reduced inflammation, fibrosis, and expression of profibrotic genes, including Col1a1, Igf1, and Mmp9.

Discussion/Conclusion: Los-mediated AT1 inhibition reduces intestinal fibrosis in CD-like ileitis. These promising results support further exploration of Los into clinical practice.

3. Correlations between liver fibrosis severity and risk factors in metabolic dysfunction-associated fatty liver disease (MAFLD)

Carmen Atodiresei (Iasi, RO)

Introduction: MAFLD is a major cause of chronic liver diseases, with the progression of fibrosis to metabolic-associated steatohepatitis (MASH), cirrhosis, and hepatocellular carcinoma. The disease progression is correlated with insulin resistance, type 2 diabetes (T2DM), dyslipidemia, obesity and cardiovascular diseases. This study analyzes the correlations between liver fibrosis severity and associated risk factors.

Methods: This retrospective study included MASH patients (January 2024–January 2025) diagnosed via ultrasound. Other MAFLD causes were excluded. All patients underwent vibration-controlled transient elastography-VCTE and controlled attenuation parameter-CAP to assess fibrosis and steatosis. Steatosis was classified as mild (LS: 248–279 dB/m) or severe (SS > 280 dB/m); fibrosis as mild (LF < 9 kPa) or severe (SF ≥ 9 kPa).

Results: A total of 150 patients were included, with a mean age of 58.4 years, predominantly male (60%). Of these, 88 patients with obesity (BMI ≥ 30 kg/m^2) – group A; 55 patients with T2DM or impaired glucose metabolism – group B; 45 patients with dyslipidemia – group C; and 35 patients with hypertension – group D. The prevalence of SS and SF was as follows: group A – SS: 36/88 (40.9%), SF: 20/88 (22.7%); group B – SS: 48/55 (87.3%), SF: 22/55 (40%); group C – SS: 32/45 (71.1%), SF: 11/45 (24.4%); group D – SS: 11/35 (31.4%), SF: 8/35 (22.9%). Additionally, 88 patients (58.7%) had only one associated risk factor – SS, SF: 0%; 51 patients (34%) had two risk factors – SS: 92.2%, SF: 27.5%; and 11 patients (7.3%) had three risk factors – SS, SF: 100%.

Discussion/Conclusion: Statistically significant correlations were found between SF-T2DM, SS-T2DM and dyslipidemia. The association of multiple risk factors correlates with severe fibrosis and steatosis. T2DM appears to be the main risk factor for severe steatosis and fibrosis. The association of metabolic factors increases both the severity of steatosis and fibrosis. Early identification of at-risk individuals may reduce complications and mortality associated with liver diseases.

4. Role of CCL5 in the pathology of hepatitis delta infection

Birke Bartosch (Lyon, FR), Enkhtuul Batbold (Lyon, FR), Olga Khomich (Lyon, FR), Jennifer Molle (Lyon, FR), Andres Roca Suarez (Lyon, FR), Xavier Grand (Lyon, FR), Alexander Ivanov (Moscow, RU), Fabien Zoulim (Lyon, FR)

Introduction: Liver cancer is the sixth most common cancer and the third most common cause of cancer-related deaths worldwide. The number of new HCC cases is predicted to increase by 55% by 2040. One main cause of liver cancer are hepatitis viruses. Among them, HBV and HCV are considered oncogenic viruses, but the role of HDV in hepatocarcinogenesis (HCC) is still unknown. Chronic hepatitis Delta is associated with accelerated fibrosis progression and increased HCC incidence compared to chronic HBV infection. Thus, it is crucial to understand the mechanisms underlying the pathophysiology of chronic hepatitis Delta. We have identified CCL5, expressed in a wide variety of myeloid and lymphoid populations within the liver microenvironment, to be induced by HDV. Importantly, increased levels of CCL5 have been implicated in the progression of chronic liver disease towards HCC in the context of several different aetiologies.

Methods: Differentiated HepaRG and PHH as well as well as other liver resident cell types were infected with HDV, HBV or both, or conditioned media derived from these infections. Infection and cellular responses were monitored by RTqPCR, single cell sequencing, western blotting, ELISA and other.

Results: In single-cell RNAseq, mono-HDV or HBV/HDV co-infected HepaRG cell transcriptomes clearly differed from non-infected and HBV-infected cells. Pathway analysis in these populations revealed strong inflammatory responses to be associated with HDV infection, particularly IFN signaling. Virus-induced IFN signalling was furthermore associated with important metabolic alterations. Furthermore, a mono-HDV infected sub-cluster of HepaRG cells showed a strong upregulation of CCL5, which was induced by HDV independently of IFN signaling. Furthermore, CCL5 produced in response to HDV infection was found to be secreted and to activate stellate cells in co-culture.

Discussion/Conclusion: Our study describes the characterization of the transcriptional profiles of HBV- and HDV-infected mono- or co-infected cell populations. It furthermore shows upregulation and secretion of chemokine CCL5 to be induced specifically in HDV mono-infected cells. HDV-induced CCL5 is secreted from hepatocytes and thus may play an important part in driving fibrosis progression. Translational studies in the future will allow to address these findings in vivo and to ask whether CCL5 may also play a role in the excessive inflammatory phenotype and increased HCC incidence, known to be associated with chronic hepatitis Delta.

5. Primary ileocecal lymphoma presented by chronic diarrhea and treated with drugs

Metin Basaranoglu (Istanbul, TR), Melilke Bilgic (Istanbul, TR)

Introduction: Primary intestinal non-Hodgkin lymphoma (PINHL) is an uncommon form of extranodal lymphoma (1–4% of all GI malignancies and 10–15% of NHL). This malignancy predominantly affects the small intestine, especially the ileum, due to its rich lymphoid tissue. PINHL often presents with non-specific gastrointestinal symptoms, making it a diagnostic challenge and often resulting in delayed diagnosis.

Methods: A 35-year-old female presented to the clinic with a 4-month history of nausea, vomiting, epigastric pain, and sometimes bloody diarrhea. She experienced subileus attack 15 days ago. She has no fever and night sweeting, but 5 kg weight loss (8% of her actual weight) within the last 4 months. She had no chronic diseases, no history of medication use, surgeries, alcohol consumption, or smoking. Abdominal examination showed noting. Abnormal laboratory results were as follows. Hb 10.3 g/d and CRP: 7.9 mg/L, LDH: 160 U/L. Both HIV and tissue transglutaminase antibody were all negative.

Results: İmmediatly a gastroscopy and a colonoscopy performed and showed that the ileocecal valve was appeared edematous, hemorrhagic and ulcerovegetant. The ileocecal valve could not be intubated due to a significant mass effect and biopsies was taken from this pathologic areas. Tuberculosis was excluded by tissue PCR-Tb and tb culture. Pathologic examination revealed that the cells consist of atypical lymphocytes with small size, folded nuclei, and dense chromatin resembling centrocytes, along with cells displaying medium to large size, round nuclei, vesicular chromatin, and prominent nucleoli typical of centroblasts morphology. Immunohistochemical stains identified CD20, CD10, Bcl2, and Bcl6 positive atypical lymphocytes. Plasma cells were polytypic with both kappa and lambda light chain expression. Nuclear C-myc expression was 70–75% positive heterogeneously. The Ki67 proliferation index was up to 80% in focal, more strongly stained areas. The pathological diagnosis was grade 3a (focal 3b) intestinal type follicular lymphoma. Oral-iv contrast-enhanced abdominal CT scan imaging showed a hypodense mass lesion extending from the ileocecal valve to the cecum and ascending colon, measuring approximately 7 cm in length and narrowing the lumen with a medial wall thickness of up to 30 mm. The patient was referred to hematology consultation. A PET-CT examination showed that there was 6 x 4.5 cm length FDG hypermetabolic mass (SUVmax 10.94) that lies the right ileocecal valve localization but no other focus of involvement was observed. CHOP chemotherapy was started. She received her first cycle on 25/06/2024. After 30 days, she is on a good condition and no subileus.

Discussion/Conclusion: This case highlights the diagnostic complexities and challenges associated with primary intestinal non-Hodgkin lymphoma (PINHL). The patient's non-specific gastrointestinal symptoms initially suggested a range of differential diagnoses, illustrating the often ambiguous presentation of this

malignancy. The immunohistochemical findings were pivotal in establishing a diagnosis of follicular lymphoma, a subtype of PINHL, characterized by CD20, CD10, Bcl2, and Bcl6 positivity and a high Ki67 proliferation index. Early referral to hematology and initiation of chemotherapy are crucial.

Treatment typically involves a combination of surgery, chemotherapy, and radiation therapy, depending on the stage and histological subtype of the lymphoma. Despite advancements in therapeutic approaches, the prognosis of PINHL varies significantly and is influenced by the disease extent and treatment response.

6. FibroScan can diagnose NASH associated cirrhosis before decompasion hepatic

Nida Bozkurt (Istanbul, TR), Nida Bozkurt (Istanbul, TR), Metin Basaranoglu (Istanbul, TR)

Introduction: Fatty liver disease is common in generel population. One in three people has fatty liver disease by transabdominal ultrasound. However, very few develop cirrhosis in practice.

Methods: A 56-year-old female patient presents with abdominal distension and pain on the right side. The abdominal distension has been a complaint for 3–4 years, while the pain, along with diarrhea, has persisted for 1 month. The diarrhea occurs 15 times a day, and the stool is black in color. Additionally, the patient experiences non-traumatic bruising, fatigue, weakness, and occasional severe itching. In the patient's medical history, she has diabetes mellitus (DM), hypertension (HT), hypothyroidism, chronic kidney disease (CKD), familial Mediterranean fever (FMF), and gallstones.

Results: The patient's body mass index (BMI) is 43.28 kg/m^2. A CT scan of the abdomen with contrast taken 10 days ago shows lobulation of the liver contours, segmental hypertrophy of the left lobe, and atrophy of the right lobe. Additionally, a lesion that measures 18 x 20 mm is seen in segments 6–7 of the liver, which shows peripheral enhancement after IV contrast. A contrast-enhanced abdominal CT scan from February 2021 indicated mild reduced density suggestive of steatosis in the liver. In laboratory tests, the following results were obtained: C-reactive protein (CRP) 29.2 mg/L, triglycerides 173 mg/dL, gamma-glutamyl transferase (GGT) 120 U/L, and glucose 110 mg/dL. The patient is suspected to have non-alcoholic fatty liver disease leading to cirrhosis, with a FibroScan cutoff value of 38.5 kPa (F4 cirrhosis) and a controlled attenuation parameter (CAP) value of 215 (grade 1 steatosis).

Discussion/Conclusion: Today, we frequently encounter cases of cirrhosis related to non-alcoholic fatty liver disease due to the increasing prevalence of obesity. Some patients present with abdominal fluid accumulation (ascites, decompensated cirrhosis, portal hypertension), while others are detected in the operating room during gallbladder surgery. For this reason, cirrhosis due to non-alcoholic fatty liver disease is known as a ''silent killer.'' In this context, we report a case of

cirrhosis associated with fatty liver disease that presented clinically with ascites in a 56-year-old patient. If patients like this one, who are obese and diabetic, underwent elastography with FibroScan at regular intervals, for example, once a year, cases could be identified before reaching an irreversible stage, thereby potentially prolonging life expectancy.

7. Decompensated liver disease: Quality improvement project

Lucianno Carneiro (Sheffield, GB), Abu Bakar Lodhi (Sheffield, GB), Ruchika Nongrum (Sheffield, GB)

Introduction: Robust post-discharge protocols are pivotal in managing the significant morbidity and mortality associated with decompensated liver disease (DLD). This quality improvement initiative evaluated and aimed to improve discharge letter compliance to the British Association for the Study of the Liver (BASL) discharge bundle; a framework designed to improve patient outcomes and reduce hospital readmission through integrated care pathways post-discharge.

Objective: This study aims to standardize post-discharge care for patients hospitalized with DLD through the implementation of an adapted BSG/BASL discharge bundle, thereby enhancing patient outcomes and facilitating effective outpatient management.

Methods: Data from the first cycle were collected retrospectively from electronic discharge letters, before the discharge bundle was introduced. This included patients admitted to the gastroenterology ward at Sheffield Teaching Hospitals (STH) with decompensated liver disease between October and November 2024. Out of 156 patients, 33 were diagnosed with decompensated liver disease. Patients who died during their hospital stay were not included in the study. Adherence to the adapted BASL discharge bundle was assessed using key elements outlined in the guidelines, including medication reconciliation, follow-up plans, dietary advice, aetiology, and signs and symptoms of decompensation. Second-cycle data collection will commence following an educational intervention targeted towards resident doctors.

Results: The initial audit of 31 discharge letters revealed significant deficiencies. Specifically, documentation rates for key elements were as follows: aetiology of liver disease, 81% (25/31); cause of decompensation, 71% (22/31); ascites, 74% (23/31); spontaneous bacterial peritonitis (SBP), 35% (11/31); date of follow-up, 32% (10/31); and dietetic advice, 6% (2/31). Importantly, escalation plans, resuscitation status, and signposting to the British Liver Trust were absent from all 31 discharge letters. The average age of patients was 56 years, with a recorded age range between 28 and 78 years. The findings reveal a notable discrepancy between current practices and the standards recommended by BASL.

Discussion/Conclusion: Initial findings of this QI revealed substantial deficiencies in discharge letter quality for patients with DLD. This can be achieved through interventions like discharge templates and education targeted towards resident doctors, aligned with the BASL discharge bundle. Subsequent cycles of this

project will focus on implementing and evaluating these interventions to achieve sustainable improvements.

8. High dimensional analysis of murine lung bleomycin time course reveals key factors contributing to inflammation, fibrosis, and resolution of injury

Stephen Christensen (Cambridge, US), Isac Lee (Cambridge, US), Wenlan Zang (Berlin, DE), Ju Wang (Cambridge, US), Kaia Gerlovin (Cambridge, US), Frank Schlerman (Cambridge, US)

Introduction: Idiopathic pulmonary fibrosis (IPF) is a chronic, progressive lung disease with a median survival of 2–3 years The pathogenesis of IPF remains largely unknown, with most human studies focusing on end-stage tissue analysis, potentially overlooking crucial factors in disease progression. The bleomycin-induced murine lung model widely used for studying fibrotic lung diseases is an acute perturbation, exhibiting three clear phases of disease: inflammation, fibrosis, and regression/resolution.

Methods: To address the need for high dimensional characterization of the model stages, we ran a longitudinal study of intra-tracheal bleomycin treatment of murine lung, analyzing eight time points of disease and healthy mice, and three timepoints of therapeutically dosed ALK5i or nintedanib.

Results: Our findings demonstrate an overlap and upregulation of the BALF biomarker TIMP1 as early as day 3, an overlapping biomarker with published human serum data. Single-cell RNA sequencing revealed increased abundance of pathogenic cell populations, with myofibroblasts and Fab5 macrophages peaking at days 14 to 21. We also uncovered alveolar macrophage gene programs specific to the inflammatory, fibrotic, and resolution phases of the model. Therapeutic inhibition of TGFb signaling via ALK5i showed an effect on myofibroblast and Fab5 macrophage polarization, and decreased activation of myriad fibroblast and myeloid populations especially at days 14 and 21, while nintedanib treatment showed minimal effect.

Discussion/Conclusion: In conclusion, these data further elucidate the utility, limits, and mechanism-specific kinetics of the bleomycin model.

9. Effect of a multi-strain probiotic formulation on the reduction of intestinal fibrosis through the modulation of TGF-β1 signalling pathways: In vitro study

Alessia Ciafarone (L'Aquila, IT), Francesca Rosaria Augello (L'Aquila, IT), Valeria Ciummo (Chieti, IT), Serena Altamura (L'Aquila, IT), Serena Artone (L'Aquila, IT), Francesca Lombardi (L'Aquila, IT), Paola Palumbo (L'Aquila, IT), Benedetta Cinque (L'Aquila, IT), Giovanni Latella (L'Aquila, IT)

Introduction: Intestinal fibrosis is a common complication of inflammatory bowel disease (IBD), and, to date, and effective and safe antifibrotic drugs are still lacking.

Transforming Growth Factor-β1 (TGF-β1), widely recognized as a key player of fibrotic process, exerts its profibrotic effects through canonical and non-canonical signalling pathways, which are potential therapeutic targets. Although probiotics have shown significant ability and efficacy to maintain and restore the integrity of the intestinal mucosal barrier, there is still a lack of information on their effect on intestinal fibrosis. This study aimed to assess the potential anti-fibrotic impact of the lysate derived from the multi-strain probiotic formulation OxxyslabTM containing 8 different strains of lactic acid bacteria and bifidobacteria, Streptococcus thermophilus; Bifidobacterium lactis DSM 32246; Bifidobacterium lactis DSM 32247; Lactobacillus acidophilus; Lactobacillus helveticus; Lactobacillus paracasei; Lactobacillus plantarum; Lactobacillus brevis, recently reclassified as Levilactobacillus brevis, on intestinal fibrosis and epithelial-to-mesenchymal transition (EMT) process using in vitro cell models.

Methods: Human CCD-18Co fibroblasts and Caco-2 intestinal epithelial cells (IECs) were used to obtain in vitro models of intestinal fibrosis and epithelial-mesenchymal transition (EMT), respectively. For the fibrosis model, CCD-18Co cells were serum-starved for 24 hours prior to treatment with TGF-β1, with or without the probiotic formulation lysate for 48 hours. While in the EMT model, Caco-2 IECs were treated with TGF-β1 in the presence or absence of the multi-strain probiotic lysate for 96 hours. To evaluate the impact of the probiotic formulation, the expression of key fibrosis markers (Collagen I, Fibronectin, and α-SMA) and EMT markers (occludin, E-cadherin, and α-SMA), as well as critical mediators of TGF-β1-induced signaling pathways (PPAR-γ, phosphorylated SMAD2/3, phosphorylated Akt, and β-Catenin), were analyzed by western blot and immunofluorescence. Additionally, TGF-β1 gene expression in the intestinal fibrosis model was quantified by RT-qPCR.

Results: Treatment with the probiotic lysate resulted in decreased expression of Collagen I, Fibronectin, and α-SMA, as well as inhibition of the Smad, Akt, and WNT/β-catenin pathways in cultures of CCD-18Co cells treated with TGF-β1. Notably, we also observed that the probiotic lysate was able to reduce TGF-β1 gene expression in activated myofibroblasts, thereby interfering with TGF-β1 neosynthesis. Furthermore, in TGF-β1-treated Caco-2 IECs, the probiotic formulation downregulated the EMT process by increasing occludin and E-cadherin expression and reducing α-SMA expression, effects which promoted the restoration of the epithelial phenotype. Overall, the probiotic formulation appeared to inhibit two of the main mechanisms of intestinal fibrosis: the activation/differentiation of fibroblasts to myofibroblasts and EMT.

Discussion/Conclusion: This specific probiotic formula represents a potential and promising candidate as an adjuvant therapy for the prevention and even the treatment of intestinal fibrosis in patients with IBD.

10. Circulating bone marrow-derived stem cells and serum stem cell factor levels in chronic hepatitis C: Relation to hepatic fibrosis and activation of hepatic stellate cells

Hayam A. El Aggan (Alexandria, EG), N.M. Farahat (Alexandria, EG), B.M. El Sabaa (Alexandria, EG), A.S. Elyamany (Alexandria, EG), R.M. Aboy Esa (Alexandria, EG)

Introduction: Bone marrow-derived stem cells (BMSCs) are pluripotent cells that can be mobilized into circulation and recruited to sites of inflammation where they promote local tissue repair. Therefore, the present work was designed to study circulating BM-derived hematopoietic stem cells (HSCs) and mesenchymal stem cells (MSCs) and serum levels of stem cell factor (SCF), a potent stem cell mobilizing factor, in patients with chronic hepatitis C (CHC) in relation to hepatic fibrosis and activation of hepatic stellate cells.

Methods: Thirty treatment-naïve patients with CHC and 15 healthy subjects were included in the study. The BM-derived HSCs and MSCs cells in fresh whole blood samples were identified as CD34+CD45+CD117+ and CD34-CD45-CD106+ cells respectively using flow cytometric assay. Serum SCF levels were measured using an in vitro enzyme linked immunosorbant assay kit. Liver biopsies were examined to assess METAVIR histological activity grade and fibrosis stage. Immunohistochemical staining of liver specimens was done using alpha-smooth muscle actin (alpha-SMA) for identification of activated hepatic stellate cells (HpSCs).

Results: Patients with CHC showed significant increases in the percentages of HSCs and MSCs in peripheral blood and serum SCF levels compared with healthy subjects ($p < 0.05$). The percentages of circulating BMSCs showed positive correlation with serum SCF levels and inverse correlations with serum aminotransferases levels, histological activity grade, fibrosis stage and intensity of activated HpSCs ($p < 0.05$).

Discussion/Conclusion: CHC is associated with mobilization of BMSCs into the circulation in parallel with an increased SCF production which may play a role in limiting hepatic necroinflammation and fibrosis during HCV-induced liver damage.

11. Increased macrophage activation marker CD163 is associated with significant liver fibrosis and metabolic derangements in hepatitis C virus-infected patients with metabolic dysfunction-associated steatotic liver disease (MASLD)

Hoda El Aggan, Sabah Mahmoud (Alexandria, EG), Nevine El Deeb (Alexandria, EG), Amany Elyamany (Alexandria, EG), Dalia Hosny (Alexandria, EG)

Introduction: Hepatitis C virus (HCV) infection is characterized by an inflammatory milieu in the liver leading to progressive fibrosis and is associated with metabolic alterations resulting in steatotic liver disease (SLD). Metabolic dysfunction-associated steatotic liver disease (MASLD) may coexist with other chronic liver diseases including HCV infection in the presence of cardiometabolic risk factors (CMRFs). Macrophage activation plays a role in inflammatory diseases and

may contribute to hepatic steatosis and fibrosis. The present study was designed to assess CD163, a macrophage activation marker, in patients with chronic HCV infection with MASLD and their relation to hepatic fibrosis and metabolic derangements.

Methods: 37 treatment-naïve patients with chronic HCV infection and 15 healthy subjects were enrolled in the study. MASLD was defined by the presence of hepatic steatosis and at least one CMRFs, exclusion of other causes of hepatic steatosis, and no or mild alcohol consumption. Serum soluble CD163 (sCD163) levels were measured using enzyme-linked immunosorbant assay. Serum high-sensitivity C reactive protein (hsCRP), a marker of systemic inflammation, was assayed. Metabolic parameters included body mass index (BMI), lipid profile, fasting blood glucose (FBG), and insulin resistance assessed by homeostatic model assessment of insulin resistance (HOMA-IR). Liver specimens were examined for METAVIR histological activity grade (HAG) and fibrosis stage and steatosis grade. Immunohistochemical staining was performed using anti-human antibodies against CD163 and alpha-smooth muscle actin (αSMA), a marker for activated hepatic stellate cells.

Results: SLD was detected in 28 (75.7%) patients, of which 22 (59.5%) patients had MASLD. Serum sCD163 levels and hepatic CD163 expression were significantly higher in HCV-infected patients with MASLD than in those without MASLD ($p < 0.001$) and were positively correlated with BMI, serum levels of total and low-density lipoprotein cholesterol, triglycerides and hsCPR, HOMA-IR, fibrosis stage, steatosis grade and αSMA expression ($p < 0.05$). The presence of MASLD was associated with significant increases in serum levels of aminotransferases, metabolic parameters, METAVIR HAG and fibrosis stage, and hepatic αSMA expression ($p < 0.01$). The receiver operating characteristic (ROC) curve showed a high diagnostic accuracy of serum sCD163 in detecting MASLD (area under the curve [AUC] = 0.994, 95% confidence interval [CI]: 0.977–1.000, $p = 0.009$) and significant liver fibrosis. (AUC = 0.940, 95% CI: 0.861–1.000, $p < 0.001$) in HCV-infected patients.

Discussion/Conclusion: Macrophage activation as evidenced with increased CD163 levels, may contribute to metabolic derangements and development of MASLD in HCV-infected patients resulting in progression of liver fibrosis. Serum sCD163 could be a useful biomarker for detecting MASLD and significant liver fibrosis during chronic HCV infection.

12. Fibrotic processes in Fuchs endothelial corneal dystrophy

Marion Fros (Cologne, DE), Nihan Demiralay (Cologne, DE), Michael Simon (Cologne, DE), Zhao Xinlei (Cologne, DE), Bachmann Bjoern (Cologne, DE), Odenthal Margarete (Cologne, DE)

Introduction: Fuchs endothelial corneal dystrophy (FECD) is an age-related, degenerative eye disease affecting the Descemet's membrane of the cornea and the underlying endothelial layer. Central endothelial cell loss and concom-

itant altered and increased extracellular matrix (ECM) composition, as well as dysfunctional endothelial pump-leak properties, ultimately lead to blurred vision and, in advanced stages, even to corneal blindness. Due to recent evidence of an additional fibrillar layer in advanced FECD and the indication of infiltrating immune cells, chronic inflammatory processes and fibrogenic processes are hypothesised to play a major role in the advanced progression of FECD.

Methods: bulkRNA-sequencing – metadata analysis, snRNA sequencing, RNA expression analysis upon cultivation on different ECM coatings, in progress: immortalisation of own FECD-cell lines deriving from fibrillar layer positive and fibrillar layer negative FECD patient sampples and validation of results on those cells.

Results: Current preliminary data of in situ analysis of a metadata bulk RNA-sequencing set of human FECD patients' explants indicate an upregulation of various ECM proteins, among them COL1A1, COL4A1, COL4A2 and FN1, as well as MMP2 and ITGA11 in comparison to healthy donor tissue. Interestingly, in vitro cell culture experiments with an immortalised FECD cell line on collagen type I coatings indicate a dose-dependent increase in expression of COL4A2, ITGA11, and MMP2, however, not of COL1A1. In addition, markers that play a relevant role during the progression of fibrosis, like endothelial to mesenchymal transition (EndMT) markers ZEB-1 and VIM and the fibroblast-activation protein FAPa, also show a significant increase in expression in the highest coating concentration of Collagen Type I. Furthermore, preliminary snRNA sequencing data of FECD fibrillar layer-positive compared comparison to fibrillar layer-negative FECD patient-derived samples indicate additional pro-fibrogenic cell populations in fibrillar layer-positive samples, that might play a further role in the deposition of a fibrillar matrix.

Discussion/Conclusion: These preliminary data point to a potential feed-back loop of high-deposited collagen type I towards advanced progression of FECD-related fibrogenic processes and signalling pathways.

13. Comprehensive analysis of mesenchymal cells involvement in mouse liver fibrosis

Wenrui Gao (Paris, FR), Haquima El Mourabit (Paris, FR), Thierry Jaffredo (Paris, FR), Sara Lemoinne (Paris, FR), Chantal Housset (Paris, FR), Nicolas Chignard (Paris, FR), Axelle Cadoret (Paris, FR)

Introduction: Liver fibrosis results from the accumulation of extracellular matrix produced in excess by myofibroblasts (MFs). In cholangiopathies, such as primary sclerosing cholangitis (PSC), fibrosis arises in the portal area from MFs originating either from portal fibroblasts (PFs) or from hepatic stellate cells (HSCs). The aim of our work is to decipher the contribution of PFs and HSCs in the portal area in biliary and non-biliary fibrosis.

Methods: We analyzed the Abcb4-/- mouse model of biliary fibrosis and the CCl4 model of non-biliary fibrosis. Mesenchymal cells were obtained from the bilio-vascular tree of control and fibrotic livers after enrichment by FACS through the

depletion of cells expressing the lineage markers of cholangiocytes (EpCAM), endothelial cells (CD31) and hematopoietic cells (CD45 and CD11b). Mesenchymal cells then underwent scRNAseq and resulting data were analyzed with Seurat v5. In a first intent analysis, scRNAseq data from control and respective liver fibrotic samples were merged for clustering. Clusters were annotated as HSCs, PFs, vascular smooth muscle cells, endothelial cells and mesothelial cells based on the expression of previously published markers. Next, data from fibrogenic cells (HSCs and PFs) from all models were extracted and merged. After clustering, fibrogenic cells were annotated as quiescent (qHSC and qPF) or myofibroblastic (mHSC and mPF) HSCs and PFs based on known markers and cell set frequency. A differential gene expression analysis was performed to identify genes that could discriminate PFs from HSCs and mPFs from qPFs.

Results: Portal mesenchymal cells were isolated from 8 weeks old Abcb4-/- mice and mice which had received intraperitoneal injections of CCl4 for 6 weeks. The amount of fibrosis was equivalent in the two models as ascertained by Sirius red staining and Col1a1 gene expression. After cell sorting and scRNAseq of mesenchymal cells from the biliovascular tree, we selected cells with gene numbers between 200 and 5,000 and with mitochondrial genes less then 5% for further analysis. We identified 28 and 20 clusters in the biliary and non-biliary fibrosis settings, respectively. Among these clusters, 21 and 10 were identified as clusters of fibrogenic cells in biliary and non-biliary fibrosis settings, respectively. Cells of the fibrogenic clusters from the two models were then merged and re-clustered into 22 different clusters. By using published markers of PFs and HSCs and cell set frequency, we could annotate 8 clusters as MFs and 12 clusters as qPFs and/or qHSCs. Uniform Manifold Approximation and Projection (UMAP) visualization was clearly distinct between fibrogenic cell populations from the biliary and non-biliary fibrosis, suggesting specific cellular processes. Differential gene expression analysis confirmed different transcriptomic profiles between the PF and HSC lineages with a total of 12,294 differentially expressed genes (DEGs). Among DEGs, we selected genes i) which were expressed in a majority of cells of the PF clusters (pct.1 > 50%) and ii) which expression was significantly higher ($p < 0.01$, logFC > 1.8) in PFs than in HSCs. Thereby, we identified four potential markers specific of the PF lineage.

Discussion/Conclusion: By combining cell isolation and scRNAseq analysis, we have gathered information on the involvement of PFs and HSCs in biliary and non-biliary fibrosis. Our approach allows for the identification of specific markers of fibrogenic cells populations preferentially implicated in biliary vs. non-biliary fibrosis.

14. Role of budesonide in improvement of the fibrosis in patients with primary biliary cirrhosis after incomplete response to UDCA monotherapy

Amelia-Valentina Genunche-Dumitrescu (Craiova, RO), Carmen-Daniela Neagoe (Craiova, RO), Carmen-Daniela Badea (Craiova, RO), Roxana Surugiu (Craiova, RO), Cristina Deliu (Bals, RO), Aurelian-Adrian Badea (Bucharest, RO)

Introduction: Aim of our study was the assessment of the effect of combined therapy (two years combined therapy with UDCA and budesonide) on histological evolution of primary biliary cirrhosis (PBC) after suboptimal response to UDCA monotherapy.

Methods: We studied 24 patients with PBC (stages I–III), with suboptimal response to UDCA monotherapy (13–15 mg/kg/day, 12 months). Due to incomplete response of this therapy, 14 patients (A group) were treated with combined therapy (UDCA 13–15 mg/kg/day and budesonide 9 mg daily divided in 3 doses) and 10 patients (B group) received increased dose of UDCA (15–20 mg/kg/day). In this comparative study we evaluated serum levels of aminotransferase, Bb, AP, liver histology, activity and fibrosis scoring (METAVIR criteria) at 6, 12 and 24 months. Also, we monitored the hepatic fibrosis by liver stiffness measurements.

Results: In both groups, clinical symptoms significant improved after 6 months (in 28.5% of cases in A group and 30% of cases in B group), in 60.7% after 12 months and 89.28% after 24 months. In B group the mean value of serum bilirubin concentration was reduced from 6.7 + 2.5 mg%, at baseline, to 2.8 + 1.3 mg% at 6 months and to 1.7 + 0.7 mg% at 12 months. Aminotransferase values were reduced more quickly comparative with bilirubin and AP levels: with 44.6% at 6 months and 63.2% at 12 months. In A group, aminotransferase values reduced more slowly, but significant decrease AP after one year ($p = 0.001$). Inflammatory activity was significantly reduced in the combined therapy (6 cases, 42.86%) and in 2 cases (20.0%) with monotherapy. In the A group fibrosis decreased in 5 cases, but only in one case in B group. After 24 months, histological stage of disease improved only in the A group (3 cases). Median values of liver stiffness measurements were correlated with histological severity of hepatic fibrosis. In the A group two patients presented hyperglycemia, two mild hirsutism and 4 osteoporosis, but in the B group we observed side-effect in only one patient (diarrhoea). Most of the side-effects appeared in patients with stage III PBC and only in two patients we reduced the budesonide dose.

Discussion/Conclusion: UDCA combined with budesonide improved liver histology and the liver enzymes whereas the effect of UDCA monotherapy was mainly on liver function tests. The association between UDCA and budesonide can represent an effective therapeutic option in treatment of PBS after suboptimal response to UDCA monotherapy.

15. Identifying microbial drivers of fibrostenotic stricturing Crohn's disease

Rabina Giri (Brisbane, AU), Anna Amiss (Brisbane, AU), Shuhang Li (Brisbane, AU), Jakob Begun (Brisbane, AU)

Introduction: Intestinal fibrosis is a key pathological process in Crohn's disease (CD), resulting in stricturing complications (B2 phenotype) that often necessitate surgery. Unlike inflammatory pathways, fibrogenesis in CD lacks targeted interventions and reliable biomarkers to identify at-risk patients during the early, clinically

silent stages. Emerging evidence implicates the gut microbiome specifically the mucosa-associated microbiota (MAM) as a potential initiator of fibrotic responses in the intestinal mucosa. However, a mechanistic link between microbial activity and intestinal fibrosis remains to be elucidated. We hypothesise that both MAM and host immune signatures in CD patients at B1 stage will predict progression to B2 behaviour, offering novel predictive biomarkers, to facilitate an early interventional treatment to prevent B2 phenotype.

Methods: To investigate microbial contributions to fibrosis, ileal biopsies were obtained from CD patients with stable inflammatory disease (B1), those who later progressed to fibrostenotic disease (B1→B2), and non-IBD controls. MAM communities were cultured ex vivo, and their secreted bioactive metabolites (secretomes) were applied to THP-1 macrophages and CCD-18Co fibroblasts to assess induction of TNF and COL1A1, respectively. Microbial composition was characterised by 16S rRNA sequencing, and functional clustering of secretome activity was performed.

Results: Microbial profiles from B1→B2 patients were distinct from those with stable B1 disease. Functional assays revealed that secretomes from progression-prone patients significantly upregulated fibrotic (COL1A1) and inflammatory (TNF) gene expression compared to controls. Importantly, microbial outgrowths could be categorised into functionally distinct groups: pro-fibrotic, pro-inflammatory, dual-active, or inert highlighting potential for early risk stratification based on microbial function rather than taxonomy alone.

Discussion/Conclusion: These findings suggest that mucosal microbiota-derived metabolites can drive fibrotic responses in intestinal tissue. Functional microbial profiling represents a promising avenue for identifying patients at risk of fibrostenotic progression and developing microbiota-targeted strategies to prevent fibrosis in Crohn's disease.

16. Comparing the use of liver fibrosis scores in MASLD/MASH and comorbidities

Iryna Hryhorchuk (Chernivtsi, UA), Larysa Sydorchuk (Chernivtsi, UA), Ruslan Sydorchuk (Chernivtsi, UA), Bohdan Lytvyn (Chernivtsi, UA), Andrii Sydorchuk (Neu-Ulm, DE), Igor Sydorchuk (Chernivtsi, UA), Mykhaylo Yarynych (Chernivtsi, UA), Iryna Sydorchuk (Siegen, DE)

Introduction: Metabolic dysfunction-associated liver disease (MASLD) ranges from simple steatosis to metabolic dysfunction-associated steatohepatitis (MASH), progressing to cirrhosis and hepatocellular carcinoma. Compared to MASLD, patients with MASH are more likely to develop advanced stages of liver fibrosis, cirrhosis and carcinoma. Whereas liver biopsy remains the gold standard for detecting liver fibrosis this procedure is both expensive and complex, causing difficulties for patients and physicians, and preventing repeated procedures. Moreover, often MASLD patients may have minor to moderate clinical picture until advanced disease, making it difficult for the clinician to decide when to perform biopsy, which result in delayed diagnosis and management of disease. Advanced

imaging methods such as elastography, computed tomography or magnetic resonance imaging have been developed to detect liver fibrosis early, but they are still relatively expensive and unavailable in limited resources settings. Most common non-invasive scoring systems for liver fibrosis are NAFLD Fibrosis Score, ELF-4, BARD, FIB-4, etc. and their numerous modifications. Each of them have both pros and cons and may be more beneficial in different clinical situations. Therefore, the aim of this study was to compare diagnostic value of the most common scoring models for prognosis of liver fibrosis in MASLD/MASH.

Methods: The retrospective cohort study enrolled 62 MASLD/MASH patients (mean age 51.91 ± 7.14 years) with comorbidities (hypertension, CAD, diabetes, and hyperlipidaemia). Most of the patients were overweight (79.03%), female gender dominated (56.45%). Clinical and laboratory data needed for calculating respective scores (liver profile, lipid profile, serum creatinine, coagulation profile, etc.) were obtained from the medical records tested within a period before/around the biopsy. Liver biopsies were examined by at least two pathologists, the extent of fibrosis was staged 0–4, with 3–4 considered advanced fibrosis (group 1) and rest – non-advanced (group 2). The distribution pattern of patients with different fibrosis stages was as follows: stage 0 – 22.58%; 1 – 19.35%; 2 – 27.42%; 3 – 16.13%; 4 – 14.52%. Scores were calculated online using MedCalc tools. The variables associated with the severity of fibrosis in univariate analyses were selected for the multivariate logistic regression (MLR) to compare diagnostic validity of different scoring models.

Results: Compared to group 1, no significant differences ($0.08 < p < 0.65$) were observed in group 2 emphasizing standard epidemiologic data (age, sex, weight, and incidence of diabetes). In addition, creatinine, triglycerides, LDL and TCL differed unreliably ($0.05 < p < 0.41$). Except AST ($p = 0.08$), group 2 patients (advanced fibrosis) showed significantly higher ALT, ALT/AST ratio, INR, bilirubin, severity of hypertension, and lower HDL ($0.0001 < p < 0.045$). MLR showed that ALT/AST ratio (OR = 1.81, 95% CI: 1.15–3.06, $p < 0.01$), INR (OR = 7.95, 95% CI: 1.93–39.27, $p < 0.01$), bilirubin (OR = 1.81, 95% CI: 1.15–3.06, $p < 0.01$), and age (OR = 0.95, 95% CI: 0.68–1.07, $p < 0.05$) were significant factors for advanced fibrosis. Other tested variables, like increased bilirubin, diabetes, and hypertension were not independently significant ($0.05 < p < 0.11$). NAFLD Fibrosis Score, ELF-4, BARD, and BARDI scores showed sensitivity 0.861, 0.735, 0.837, and 0.871; specificity 0.561, 0.583, 0.635, and 0.622, respectively. Both positive and negative prognostic values for all scores ranged between 0.349–1.00 and 0.689–1.00.

Discussion/Conclusion: It has been shown previously that liver biopsies are the golden standard for liver fibrosis diagnosis, whereas being expensive and invasive. A set of imaging methods have been developed demonstrating superior or even comparable results to clinical scoring models. For instance, for the transient elastography, the AUROC was reported to be 0.9047–0.94. Anyway, imaging techniques remain more expensive and available in specialized centres only. It becomes evident that most common non-invasive liver fibrosis scores may have potential for mistakes and cannot substitute both liver biopsies and ultrasonography. However, combination of different scoring models may poten-

tiate their prognostic efficacy and decrease risk of miscalculations. Therefore, we recommend using a set of several scores to multiply beneficial effect and alleviate possible mistakes.

17. Metabolic dysfunction-associated steatotic liver disease is a risk factor for the development of liver fibrosis in patients with multiple myeloma undergoing chemotherapy

Ganna Maslova (Poltava, UA), Elizaveta Stadnik (Poltava, UA)

Introduction: Patients with multiple myeloma (MM) are frequently diagnosed with concomitant metabolic dysfunction-associated steatotic liver disease (MASLD). Liver fibrosis that develops in the setting of MASLD and concurrent cytotoxic therapy is considered an unfavorable prognostic factor.

Methods: The aim: To investigate the role of MASLD in potentiating the risk of cytostatic-induced liver fibrosis in patients with MM who received a single line of chemotherapy.

22 MM patients (12 (54.6%) female, 10 (45.4%) male), age 65.1 ± 1.67 years who had completed a course of chemotherapy six months earlier and had achieved a response to treatment were examined. According to the Durie-Salmon classification, all patients were diagnosed with stage IIIA disease. Based on the International Staging System, stage I was found in 9.1% (2/22), stage II in 54.5% (12/22), stage III in 36.4% (8/22). The hematological panel included platelet count. The biochemical panel involved the assessment of alanine aminotransferase (ALT), aspartate aminotransferase (AST), total cholesterol, high-density lipoproteins (HDL), low-density lipoproteins (LDL), triglycerides. The probability of liver fibrosis was assessed using the FIB-4 score. The control group of practically healthy individuals (HC) consisted of 16 persons with a mean age of 28.0 ± 1.1 years.

Results: The patients were divided into two groups depending on the presence of MASLD: I (n = 10) – undergoing maintenance therapy for MM with concomitant MASLD; group II (n = 12) – undergoing maintenance therapy for MM without concomitant MASLD. All patients with concomitant MASLD had either overweight or obesity. Platelet levels did not differ significantly between the two groups or HC. In group I patients, ALT and AST activity increased by 1.6-fold ($p < 0.05$) and 1.6-fold ($p < 0.05$), compared to group II, and by 1.7-fold ($p < 0.05$) and 1.5-fold ($p < 0.05$), respectively, compared to the HC. In group II, ALT and AST activity did not significantly differ from the HC. Dyslipidemia due to elevated LDL levels was observed in 60% (6/10) of group I and in 8.3% (1/12) of group II. FIB-4 score > 1.45 was found in 80% (8/10) of group I, in 33.3% (4/12) of group II ($\chi^2 = 4.79$, $p < 0.05$). Importantly, all patients had a FIB-4 score <1.45 prior to initiating specific chemotherapy courses.

Discussion/Conclusion: The presence of MASLD potentiates the formation of liver fibrosis on the background of chemotherapy in patients with MM.

18. Evaluation of liver fibrosis in patients with NAFLD and cutaneous psoriasis compared to patients with NAFLD

Carmen Daniela Neagoe (Craiova, RO), Simona Laura Ianosi (Craiova, RO), Vlad Neagoe (Craiova, RO), Amelia Genunche-Dumitrescu (Craiova, RO), Mihaela Popescu (Craiova, RO), Anca-Maria Amzolini (Craiova, RO)

Introduction: Patients with NAFLD and psoriasis have an increased risk of developing advanced fibrosis compared to patients with NAFLD only, due to chronic low-grade inflammation and metabolic abnormalities.

Aim of our study was to compare the sensibility and specificity of the non-invasive scores and liver biopsy in determining fibrosis in patients with NAFLD and moderate to severe psoriasis.

Methods: The study group was constituted of 50 patients: 18 patients with psoriasis and NAFLD forming the Pso group and 32 patients with NAFLD, as NAFLD group. Inclusion criteria: over 18 years of age, with NAFLD, +/- moderate to severe psoriasis and no hepatotoxicity treatment in the last two years or other causes of hepatic steatosis. The following scores were calculated: BARD score, Fibrosis-4 (FIB-4) score, and NAFLD fibrosis score (NFS). Liver biopsy was performed in all patients.

Results: Statistically significant differences were recorded regarding age, AST, albumin and number of platelets between group with advanced fibrosis and those groups with no/mild fibrosis (F0, F1), so that patients with advanced fibrosis were older, with a higher level of AST and a low serum level of albumin and platelet count. Fibrosis was slightly increased in Pso group compared to NAFLD group (61.11% vs. 59.37%), but if we evaluated the patients in terms of fibrosis degree, we found that the high degree of fibrosis is significantly larger in the Pso group (72.7%) than in control group (31.57%).

By calculating Kendall's test, we also observed a strong direct correlation between the degree of fibrosis and FIB-4 (tau = 0.558) and NFS (tau = 0.490) scores, with a critical statistical impact, and the lack of a correlation with the BARD score (tau = 0.095; p = 0.332).

Discussion/Conclusion: Severe fibrosis was more frequent in Pso group. The non-invasive tests are most useful for confirmation of the advanced stages of the disease. The NFS score proved a high statistically significant correlation ($p < 0.0001$) with the fibrosis histological lesions.

19. Differential risk of dysplasia in small-duct versus large-duct primary sclerosing cholangitis in IBD patients: A retrospective study

Nilanga Nishad (Sheffield, GB), Sreedhar Subramanian (Cambridge, GB), Sarala Janarthanan (Cambridge, GB), Mo Thoufeeq (Sheffield, GB)

Introduction: Inflammatory Bowel Disease (IBD) patients with concurrent primary sclerosing cholangitis (PSC) are at a much higher risk of dysplasia and colorectal

cancer (CRC) but risk factors remain poorly defined. It is unclear if patients with small-duct PSC (sdPSC) are at a similar risk to large-duct PSC (ldPSC). We sought to evaluate the development of dysplasia among patients with sdPSC vs. ldPSC.

Methods: We identified PSC patients from an electronic registry of IBD patients treated at Cambridge University Hospital NHS trust from 2010 to 2024. We retrospectively collected surveillance colonoscopy, histological, IBD and PSC data as part of an institutional audit. Histological samples were evaluated over time to identify presence of dysplasia among patients with sdPSC vs. ldPSC. Kaplan Meier survival curve with Mantel-cox log rank test was used to compare the development of dysplasia among the two groups. Clinical and endoscopic variables associated with dysplasia was also compared.

Results: There were 117 patients with IBD-PSC, sdPSC 16 (14%), ldPSC 101 (84%). Among them 84 (72%) UC, 23 (20%) CD and 10 (8%) IBD-U. Mean age was 44.9 (41.3–52.5) years and there were 73 males (62%). The mean (s.d.) age, duration from diagnosis of PSC, of the sdPSC vs. ldPSC were 46 (20) vs. 45(19) ($p = 0.8$) and 9 (8) vs. 11 (6) years ($p = 0.5$). Nine patients with ldPSC (9%) vs. none of the sdPSC developed low grade dysplasia ($p = 0.3$). There were no patients with high-grade dysplasia or colorectal cancers. Among the patients with dysplasia all had UC pancolitis. Survival analysis did not show a statistical significance with respect to development of dysplasia dependent on the type of subtype of PSC. (Mantel -cox log rank value = 0.64, $p = 0.42$) (Figure 1) Patients with LGD were more likely to be older (58 vs. 44 years ($p = 0.02$) and have a longer disease duration of IBD (25 years vs. 15 years, $p = 0.03$) whereas duration of PSC was not different (11 vs. 10 years, $p = 0.8$)

Discussion/Conclusion: ldPSC is associated with development of low-grade dysplasia. Patients with LGD were more likely to be older and have longer disease duration of IBD. There were no instances of dysplasia within the sdPSC cohort. Our findings need to be validated in larger cohorts.

20. Smart phone application to exclude varices in compensated cirrhosis with liver transaminases, liver and splenic stiffness using transient elastography

Nilanga Nishad (Sheffield, GB), Madunil Niriella (Ragama, LK), Arjuna De Silva (Ragama, LK), Gayan Hewathanthri (Colombo, LK)

Introduction: We used AST to ALT ratio (AAR) and, liver stiffness measurement (LSM), splenic stiffness measurement (SSM) by transient elastography to develop a statistical model and present it as a user-friendly smartphone application to exclude the presence of oesophageal and cardio-fundal varices to avoid upper gastrointestinal endoscopy in selected patients.

Methods: A prospective study was carried out among patients with Child-Pugh Class A cirrhosis (non-viral and BMI < 30 kg/m2). LSM and SSM were obtained using Fibroscan (EchoSens) by a single operator, blinded to the presence or absence of varices. The predictors used to develop the formula were AAR, LSM

and SSM. Multiple logistic regression was used to create the algorithms in 70% of the sample and validated using 30% of the sample with Bootstrapping of 1000. Best algorithms with the highest area under the curve (AUC) were selected and identified as different cut-off levels to exclude or predict the presence of varices. Those values were included in a smartphone application on android and iOS web-based platforms.

Results: One hundred and nine out of 211 had varices. After modelling different combinations, logistic regression formula (LRF) = 5.577 (LSM*0.035)+(SSM*0.08)+(AAR*1.48) resulted AUCs 0.93. Cut-off value < -1.26 of LRF predicted the exclusion of varices with a negative predictive value of 90%. Cut-off value > 0.829 of LRF predicted the presence of varices with a positive predictive value of 91%. Multiple values were used to develop a smartphone app on the Angular 2+ platform. (It can be downloaded for use @https://mediformula-65ef0.web.app/).

Discussion/Conclusion: The new formula using AAR, LSM and SSM can be used to predict exclusion of varices with high accuracy in non-obese patients with compensated cirrhosis of non-viral aetiology based on the patient's biochemical or fibroscan values. The smartphone application derived from this model is easy to use. It is the first mobile application to be used to exclude or predict the presence of varices utilizing SSM.

21. Plectin loss disrupts mechanotransduction and attenuates hepatic stellate cell activation

Srikant Ojha (Prague, CZ)

Introduction: Fibroproliferative disorders contribute to nearly 45% of all deaths and are often driven by chronic inflammation that predisposes to liver cancer and metastasis. In liver pathology, hepatic stellate cells (HSCs) are the principal effectors of fibrosis. In their quiescent state, HSCs exhibit a characteristic star-like morphology. Upon liver injury, increased tissue stiffness activates mechanosensitive signaling pathways in HSCs, promoting their transdifferentiation into myofibroblasts. These activated HSCs deposit excessive extracellular matrix (ECM), further enhancing tissue rigidity and reinforcing a pathological feedback loop.

Methods: To interfere with HSC mechanotransduction and halt fibrotic progression, we targeted plectin, a cytolinker protein essential for integrin-mediated mechanical signaling. We generated an HSC-specific plectin knockout (KO) mouse model using Cre-negative littermates as wild-type (WT) controls. Fibrotic responses were assessed in vivo using two clinically relevant models of liver injury: carbon tetrachloride (CCl_4) and thioacetamide (TAA). ECM deposition was quantified to compare fibrosis severity between genotypes. Additionally, primary HSCs from WT and KO mice were isolated at quiescent and activated stages for in vitro phenotypic analysis. To uncover affected molecular pathways, single-cell transcriptomic profiling was performed on primary HSCs.

Results: Plectin-deficient mice exhibited significantly reduced ECM deposition in both CCl_4- and TAA-induced liver injury models, alongside accelerated fibrosis

resolution following toxicant withdrawal. In vitro, KO HSCs displayed impaired migration and proliferation, indicating a diminished activation phenotype. Furthermore, plectin-deficient HSCs showed fewer focal adhesions, suggesting attenuated mechanosignaling as a likely mechanism underlying their reduced activation. Single-cell transcriptomic analysis identified distinct unactivated and activated HSC clusters in UMAP space. Differential gene expression analysis revealed that KO HSCs downregulated myofibroblast-associated genes while upregulating markers of quiescence, corroborating the in vivo and in vitro findings.

Discussion/Conclusion: Our study reveals a central role for plectin in HSC mechanotransduction and fibrogenic activation. Using a preclinical model, we demonstrate that disrupting plectin function dampens fibrotic signaling and ECM accumulation, highlighting plectin as a promising therapeutic target to combat liver fibrosis and its pathological sequelae.

22. Hepatocellular carcinoma surveillance at Bradford Royal Infirmary – A single centre AUDIT of surveillance outcomes

Muhammad Salman (Bradford, GB)

Background: Hepatocellular carcinoma (HCC) has a rising incidence and mortality in the UK. Improved survival is best affected by early diagnosis, hence NICE recommends six-monthly ultrasound surveillance. HCC surveillance is costly, and its effectiveness and format is debated. This audit aimed to evaluate the outcomes of HCC surveillance at Bradford Royal Infirmary.

Method: A single centre audit of hepatocellular carcinomas diagnosed between 2013 and May 2023 from MDT data. Initial dataset of 158 patients. Benign neoplasms discussed at MDT were excluded from our study (n = 19). Data from 38 cases were not available as they predated our electronic patient record and they were excluded. A further 31 cases were excluded due to significant irresolvable data gaps. In total, 70 cases were included. Statistical analyses with Chi-Square test with statistical significance set at $p < 0.05$.

Results: There were seventy HCC patients, of whom 56 were male (80%, mean age 71.1 years, age range 49.03–90.76) and 14 were female (20%, mean age 69.72, age range 48.12–88.00). 71.4% of patients were White (n = 50) and 28.6% Asian (n = 20).

The underlying liver disease was: Undiagnosed or no liver disease (25.7%, n = 18), hepatitis C (HCV, 24.3%, n = 17), alcohol-related liver disease (ARLD, 21.4%, n = 15), metabolic dysfunction-associated steatotic liver disease (MASLD, 17.1%, n = 12), hepatitis B (HBV, 5.71%, n = 4), primary biliary cirrhosis (PBC, 2.86%, n = 2), haemochromatosis (1.43%, n = 1), and cardiac cirrhosis (1.43%, n = 1).

Eighteen patients (25.7%) received potentially curative treatment (resection, ablation, or transplant). 70 patients were treated as follows: TACE (n = 12, 17.1%), ablative therapies (n = 9, 12.9%), resection (n = 7, 10%), chemotherapy (n = 4, 5.71%), and transplant (n = 2, 2.86%).

12.9% of patients (n = 9) had a biopsy of their liver lesion.

Nineteen HCC (27.1%) were detected in patients who were on an HCC surveillance programme. Mean lesion size was 3.22 cm (1.20–10.0 cm). In patients not on the surveillance programme (n = 51, 72.9%), mean lesion size was 6.87 cm (1.40–18.2 cm).

HCC patients enrolled in surveillance were significantly more likely to have a lower radiological staging grade at diagnosis than HCC patients not enrolled in surveillance. 89.5% of the surveillance cohort (n = 17) were T1a/T1b/T2 at diagnosis, compared to 45.1% of the non-surveillance cohort (n = 23), p = 0.000849.

Our patients diagnosed with HCC whilst in surveillance were also significantly more likely to receive potentially curative treatments (resection, ablation and transplant) than patients not enrolled in surveillance (52.6% vs. 15.7%, p = 0.00166). Further, HCC patients enrolled in surveillance had a significantly greater rate of survival at 9, 12 and 24 months (9-month survival: 78.9% vs. 52.9%, p = 0.0482, 12-month survival: 73.9% vs. 46.8%, p = 0.0471, 24-month survival: 64.7% vs. 35.9%, p = 0.0462).

There was significantly more viral disease in the surveillance cohort (n = 12, 63.2%) than the non-surveillance cohort (n = 9, 17.6%), p = 0.00022. Further, there was significantly more HCV-related HCC detected in the surveillance population than the non-surveillance population. HCV represented 42.1% of surveillance detected HCC (n = 8), versus 13.7% (n = 7) of the non-surveillance cohort, p = 0.0101). This represents successful enrolment of viral disease into HCC surveillance, highlighting the success of HCV management at BRI.

For the eighteen HCC patients with undiagnosed or no liver disease, the mean lesion size was 9.6cm (3.4–18.2 cm), the mean age was 77.77 (54.78–90.76), and survival rate was 57.8% at 9-months (11/19), 47.1% at 12-months (8/17) and 21.4% at 24-months (3/14).

Conclusion: Most cases of HCC at Bradford Royal Infirmary were diagnosed outside of surveillance with 27.1% surveillance-detection rate; similar to that of other UK retrospective cohort studies.

HCC patients enrolled in surveillance were significantly more likely to have an earlier stage of disease at diagnosis, significantly more likely to receive potentially curative treatment, and significantly more likely to be alive at 9-, 12- and 24-months, than HCC patients not enrolled in surveillance.

Interestingly, a significant proportion of HCC cases were made in patients with undiagnosed or no chronic liver disease. Further, HCV-related HCC was significantly more represented in the surveillance cohort representing the successful enrolment of viral disease into HCC surveillance and highlighting the success of HCV management at Bradford Royal Infirmary.

23. Fibrosis and steatosis assessment in chronic hepatitis B: Correlation with viral replication

Georgiana Elena Sarbu (Iasi, RO), Alina Ecaterina Jucan (Iasi, RO), Claudiu Vasile Mihai (Iasi, RO), Ioana Ruxandra Mihai (Iasi, RO), Carmen Atodiresei (Iasi, RO), Andreea Lungu (Iasi, RO), Otilia Nedelciuc (Iasi, RO), Mihaela Dranga (Iasi, RO), Cristina Cijevschi Prelipcrean (Iasi, RO), Catalina Mihai (Iasi, RO)

Introduction: Chronic hepatitis B (CHB), often progressing to cirrhosis and hepatocellular carcinoma, is a major cause of liver-related mortality. This study aims to assess the patterns of hepatic fibrosis (F) and steatosis (S) in patients with CHB.

Methods: We retrospectively included HBsAg-positive patients with HBV DNA > 2000 IU/mL with ultrasound confirmed hepatic steatosis, evaluated between 2023–2024 in a tertiary center. All underwent transient elastography with controlled attenuation parameter (CAP) measurement for antiviral therapy eligibility. S and F were defined as follows: S0–S1 150–260 dB/m for low steatosis (LS), S2–S3 > 260 dB/m for significant steatosis (SS), F0–F2 2–9.5 kPa for low fibrosis (LF), and F3–F4 > 9.5 kPa for advanced fibrosis (AF).

Results: A total of 98 patients were enrolled (mean age: 57 years; M:F ratio = 67:31). Among them, 70.4% had LS, 29.6% had SS, 68,4% had LF and 31.6% had AF. Based on viral load, 57 (58.2%) were classified into Group A (HBV DNA 2000–600,000 IU/mL) and 41 (41.8%) into Group B (HBV DNA > 600,000 IU/mL). In Group A, 56.1% had LS, 43.8% had SS, 73.6% had LF and 26.3% had AF; in Group B, 90.2% had LS, 9.7% had SS, 60,9% had LF and 39% had AF. A statistically significant association was observed between high viremia and low steatosis ($\chi^2 = 13.3$, $p < 0.001$). In contrast, the association between viremia and fibrosis was not statistically significant ($\chi^2 = 1.7$, $p = 0.182$).

Discussion/Conclusion: Our findings suggest that lower hepatic steatosis is associated with higher levels of viremia, indicating a potential inverse relationship between viral replication and hepatic fat accumulation. No significant correlation was found between viral load and fibrosis grade.

24. Stage-specific drivers of clinical progression in advanced chronic liver disease

Georg Semmler (Vienna, AT), Benedikt Simbrunner (Vienna, AT), Marta Bofill Roig (Barcelona, ES), Elias Meyer (Vienna, AT), Lorenz Balcar (Vienna, AT), Mathias Jachs (Vienna, AT), Lukas Hartl (Vienna, AT), Benedikt Silvester Hofer (Vienna, AT), Georg Kramer (Vienna, AT), Paul Thoene (Vienna, AT), Christian Sebesta (Vienna, AT), Nina Dominik (Vienna, AT), Rodrig Marculescu (Vienna, AT), Peter Quehenberger (Vienna, AT), Bernhard Scheiner (Vienna, AT), Philipp Schwabl (Vienna, AT), Albert Friedrich Staettermayer (Vienna, AT), Michael Trauner (Vienna, AT), Thomas Reiberger (Vienna, AT), Mattias Mandorfer (Vienna, AT)

Introduction: Advanced chronic liver disease (ACLD) encompasses diverse pathophysiological mechanisms that evolve during disease progression. We

analyzed the clinical course of ACLD using a multistate framework and evaluated the stage-specific prognostic relevance of biomarkers representing key pathogenic mechanisms.

Methods: In a prospective cohort of 464 ACLD patients undergoing hepatic venous pressure gradient (HVPG) measurement (2017–2021), clinical stages were categorized as compensated ACLD (cACLD), first decompensation, further decompensation/acute-on-chronic liver failure (ACLF), liver-related death (LRD), and recompensation. Stage transitions over a median follow-up of 29 months were modeled. Baseline biomarkers included markers of portal hypertension (HVPG), endothelial dysfunction (VWF), fibrogenesis (ELF), liver function (MELD, albumin, bile acids), systemic inflammation (CRP, IL-6, procalcitonin), and circulatory dysfunction (proBNP, copeptin).

Results: At 24 months, 12% of cACLD patients progressed to first decompensation. Among those with decompensated cirrhosis, 19% developed further decompensation/ACLF at 12 months, and of those with further decompensation, 33% experienced LRD. Biomarker relevance varied by stage: in cACLD, portal hypertension (HVPG), fibrogenesis (ELF), and liver function (albumin) were indicative of disease progression, shifting towards systemic inflammation (CRP) and liver function (albumin) in decompensated cirrhosis, with the additional contribution of circulatory dysfunction (copeptin) in further decompensation. Network analyses confirmed a stage-dependent shift in biomarker interconnectivity, from portal hypertension and fibrogenesis in early stages to inflammatory and circulatory drivers in advanced disease.

Discussion/Conclusion: The prognostic landscape of ACLD is dynamic, with distinct biomarker profiles dominating at different disease stages. Strategies targeting portal hypertension and liver fibrosis are most relevant in cACLD, while inflammation and circulatory dysfunction gain importance after decompensation. These insights support stage-tailored interventions and biomarker-guided personalization of care in ACLD.

25. Ischemic heart disease is associated with liver fibrosis in patients with metabolic dysfunction-associated steatotic liver disease

Igor Skrypnyk (Poltava, UA), Ganna Maslova (Poltava, UA), Inna Pilat (Poltava, UA), Vladyslav Ostrovskyi (Poltava, UA)

Introduction: Formation of metabolic dysfunction-associated steatotic liver disease (MASLD) is accompanied by a high risk of development of ischemic heart disease (IHD), which can be associated with progression of liver fibrosis.

Methods: The aim: to analyze the relationship between the presence of IHD and liver fibrosis according to the FIB-4 in patients with MASLD.

46 patients with MASLD were examined. The ratio men/women was 31 (67.4%)/15 (32.6%), age range – 25–72 years. IHD was detected in 24 (52.2%) patients (stable angina I–II functional class, diffuse cardiosclerosis). MASLD patients were

distributed into groups: I (n = 22) –without concomitant IHD, II (n = 24) – with concomitant IHD. Anthropometric measurements, including the determination of body mass index (BMI), were provided to all patients. Complete blood count parameter, blood biochemistry test parameters were determined. The FIB-4 index was calculated.

Results: The age of patients of group II was 1.2 times higher than that of group I (p = 0.002). BMI in patients of group I was 33.19 ± 6.69 kg/m2, group II – 3.19 ± 6.69 kg/m2 without a significant difference between the groups (p > 0.05). Platelet count in group I was 250.8 ± 79.08 × 109/l, in group II – 227.2 ± 67.33 × 109/l (p > 0.05). Blood biochemistry parameters had no significant difference between groups I and II (p > 0.05). FIB-4 index in patients of group II was 1.5 times higher than that of group I. FIB-4 index in group I in the range of 1.3–2.67 and greater than 2.67 was detected in 3 (13.6%) and 1 (4.5%) patients, in group II in the range of 1.3–2.67 and greater than 2.67 was detected in 6 (25%) and 3 (12.5%) patients respectively (p> 0.05).

Positive correlations between FIB-4 index and AST activity (r = +0.57; p = 0.004), FIB-4 index and total bilirubin (r = +0.48; p = 0.02) and negative correlation between FIB-4 index and platelet count (r = -0.64; p = 0.001) were detected in patients of group II.

Discussion/Conclusion: According to the results of our study, patients with MASLD and concomitant IHD have an increased risk of liver fibrosis development.

26. Transient elastography and non-invasive fibrosis scores in infantile lysosomal acid lipase deficiency (Wolman disease)

Mordechai Slae (Jerusalem, IL), Eyal Shteyer (Jerusalem, IL)

Introduction: Transient elastography is an emerging technique in the assessment of liver stiffness in patients with liver disease. Based on shear wave technology, this noninvasive imaging study produces indices of liver fibrosis, potentially replacing the more invasive follow-up test of liver biopsy or MRI-elastography, which in children commonly requires anesthesia.

In pediatric patients, it has been used to assess liver status in congenital and acquired liver disease. In addition, it has been reported and proposed as a tool for follow-up of liver storage diseases such as Wilson disease, since accumulated material in the liver can also cause liver stiffness. Follow-up of liver stiffness showed improvement with chelation therapy. Other non-invasive fibrosis evaluations include APRI score, FIB-4 score and AST/ALT ratio score.

Infantile lysosomal acid lipase deficiency (LAL-D), or Wolman disease, is a rare genetic storage disease. Mutations in the LIPA gene cause dysfunction of the lysosomal acid lipase enzyme which metabolizes triglycerides and cholesterol esters, resulting in liver, intestinal and immune-cells storage, deficiency of HDL and excess of cholesterol and LDL. Without treatment, the disease is lethal. Other complications include failure to thrive, anemia, malnutrition and Hemophagocytic

Lymphohistiocytosis (HLH), caused by cholesteryl ester-induced inflammasome activation in macrophages. There is a milder form of LAL-D in which the mutations cause milder disease in older children and adults.

Recently, enzyme replacement therapy (ERT) has been developed, and patients receiving this treatment become stable; however, adjustment of enzyme dose and dietary management are frequently required. All patients are instructed to keep a low fat diet.

The need to assess liver status is very important in managing this liver disease. Given the invasive nature of liver biopsy, there is a risk that it will be avoided in assessment of disease course, leading to suboptimal management and decreased treatment success.

Methods: We compared the results of transient elastography to other non-invasive fibrosis scores, including APRI score, FIB-4 score and AST/ALT ratio score, in 4 cases of Wolman disease, and potential relation between severe score and a complication of the disease which affects the liver, namely HLH.

Results: Four children with Wolman disease have been followed since the neonatal period. All were diagnosed at approximately 2 months of age, and their current ages range from 2 years and 1 month to 6 years and 10 months. Diagnosis was confirmed by reduced enzymatic activity and/or identification of known pathogenic mutations in the LIPA gene. All patients presented with adrenal calcifications and were treated with enzyme replacement therapy (ERT) using sebelipase alfa.

All four patients developed hemophagocytic lymphohistiocytosis (HLH), either at initial presentation (in all cases) or, in two patients, during the disease course despite ongoing ERT.

Transient elastography (FibroScan) was performed in all patients. Two patients had mild fibrosis (F1) with liver stiffness measurements of 5.3 and 6.4 kPa at ages 8 and 32 months, respectively. One patient had moderate fibrosis (F3; 10.5 kPa at 64 months) and underwent liver biopsy, which confirmed an Ishak fibrosis score of F3. The fourth patient showed advanced fibrosis (F4; 16.1 kPa at 20 months).

FibroScan liver stiffness measurements (kPa) and fibrosis stage (F score) correlated strongly with the APRI score ($r = 0.97$ and $r = 0.92$, respectively), but not with the FIB-4 index or the AST/ALT ratio. FibroScan results did not correlate with HLH episodes during ERT, whereas total cholesterol levels and FIB-4 scores were positively correlated with HLH development ($r = 0.90$ and $r = 0.92$, respectively).

Discussion/Conclusion: Transient elastography appears to be a useful non-invasive tool for assessing liver involvement in patients with Wolman disease, showing good correlation with the APRI score. In contrast, the FIB-4 index does not correlate with liver stiffness but may serve as a potential marker for predicting the development of secondary HLH during enzyme replacement therapy.

27. Intestinal fibrosis in IBD: Linkage with opportunistic infections, mesenteric vessels endothelial dysfunction and colonic resistance may have possible genetic background

Andrii Sydorchuk (Neu-Ulm, DE), Larysa Sydorchuk (Chernivtsi, UA), Bohdan Lytvyn (Chernivtsi, UA), Ruslan Sydorchuk (Chernivtsi, UA), Mykhaylo Yarynych (Chernivtsi, UA), Iryna Sydorchuk (Siegen, DE), Igor Sydorchuk (Chernivtsi, UA), Petro Kyfiak (Chernivtsi, UA)

Introduction: IBD incorporating Crohn's disease (CD) and ulcerative colitis is commonly realized through metabolic and immune mechanisms involving vascular and digestive systems injury. The incidence of CD, compared to ulcerative colitis is almost similar, with about 20–30 cases per 100,000 populations in Western countries. Immune system has strong influence on colonic epithelium and endothelium and may have strong molecular-genetic background. Number of studies have made it possible to locate various components responsible for the genetic predisposition of the occurring CD. Among them, NOD2, TG16L1, PTPN22, IRGM and CLEC7A are most commonly directly associated with IBD. However, there is lack of data connecting genetics, vascular-endothelial changes and colonic changes including dysbiosis and inflammation. The aim of this study is to find possible connections of the endothelial function and mesenteric vessels remodelling depending on A1166C polymorphism of angiotensin II type 1 receptor (AGTR1) gene in IBD patients with fibrosis and colonic dysbiosis as a background for opportunistic infection and vascular-endothelial injury as well.

Methods: Observational study includes 104 CD patients with colonic dysbiosis in remission or mild disease at the time of investigation (CDAI score less than 150–200). For diagnosis of fibrosis we used a set of approaches, clinical history (cramping, vomiting, dietary restrictions, abdominal pain after food intake and duration of postprandial pain, abdominal distention), previous contrast-enhanced abdominal MRI/CT enterography, intestinal ultrasonography and endoscopic mucosal biopsy (graded 0–3). Standard aerobic and anaerobic microbiology techniques with nosology identification and quantity composition of microbiota were used. Intimae-media thickness (IMT) of abdominal aorta (AO) and other flow mediated parameters of mesenteric vessels evaluated sonographically. NO (nitrite/nitrate) plasma concentration, vascular adhesive molecule (sVCAM-1) level was defined by IEA. AGTR1 (A1166C) genes polymorphisms assessed in PCR.

Results: Clinical history of all patients was inconclusive, making it impossible to differentiate patients with fibrosis. Endoscopic examination showed significant narrowing of the lumen in only 6.73% of the patients, whereas bioptates showed mostly signs of mild inflammatory changes like neutrophil infiltration, mucosal erosion, lymphoid aggregates and mucosal oedema. Surprisingly, 58.65% of biopsies demonstrated fibrosis grades above 0 even in clinically absent stenosis. The microbial overgrowth syndrome of II–IV degree detected in 95.1–95.9% of cases. CC-genotype carriers of AGTR1 gene had heavier dysbiosis of III–IV grades. Patients with A-allele, had lower frequency of dysbiosis ($p = 0.004$) and moderate severity ($p = 0.037$). CC genotype of AGTR1 gene characterized by elimination

of obligate colonic indigenous constant microorganisms and contamination by pathogenic (E. coli Hly+) and opportunistic (Proteus), Enterobacteriaceae, Peptococci, Clostridium and Candida fungi. In patients with CC genotype of the AGTR1 gene a significant reduction of Bifidobacteria (35.7%, $p < 0.001$), Lactobacilli (24.1%, $p < 0.01$) and enterococci (1.5%) was found. On this background, significant increase of enterotopathogenic Escherichiae (8.94 ± 0.08 lg CFU/g), opportunistic Enterobacteriaceae (8.78 ± 0.11 lg CFU/g), Hafniae (8.69 ± 0.09 lg CFU/g), Proteus – by 55.2%, Staphylococci (5.92 ± 0.14 lg CFU/g), Candida fungi (5.60 ± 0.10 lg CFU/g) was observed.

Discussion/Conclusion: This study demonstrates difficulties and uncertainty of diagnosing intestinal fibrosis, compared to biopsies, other non-invasive methods were unable to diagnose mild fibrosis. The CC genotype of AGTR1 gene is generally characterized by elimination of normal colonic autochthonous obligate microflora and contamination by pathogenic, opportunistic and conditionally pathogenic microorganisms. The mechanism possibly involves changes of mesenteric arteries and endothelial function and may predict failures of both standard and faecal transplant therapies. This study has multiple limitations, including contingent selection, methods used and duration of the study itself.

28. Genetically determined linkage of leptin, fibrosis, and hepatic dysfunction in MASLD

Larysa Sydorchuk (Chernivtsi, UA), Bohdan Lytvyn (Chernivtsi, UA), Ruslan Sydorchuk (Chernivtsi, UA), Andrii Sydorchuk (Neu-Ulm, DE), Mykhaylo Yarynych (Chernivtsi, UA), Iryna Sydorchuk (Siegen, DE), Iryna Hryhorchuk (Chernivtsi, UA), Igor Sydorchuk (Chernivtsi, UA)

Introduction: Number of experimental and clinical studies suggest that leptin (adipokine responsible for regulating body weight and energy expenditure) plays a key role to balance energy expenditure and nutritional status in the immune system. Deposition of extracellular matrix causes damage to tissues, which will eventually lead to tissue and organ fibrosis. MASLD often leads to inflammatory damage to hepatocytes, closely related to metabolic syndrome, obesity, insulin resistance, type 2 diabetes mellitus, arterial hypertension, and fibrosis. Common mechanisms for hepatic steatosis include reduced synthesis of very low density lipoprotein, and increased triglyceride synthesis; inflammation may result from lipid peroxidative damage to cell membranes, stimulating hepatic stellate cells, leading to liver failure and fibrosis. Although the roles of leptin in obesity and diabetes have been extensively investigated, the influence of leptin on liver fibrosis is controversial and still not fully understood. Existing data on leptin linkage with fibrosis is confusing, it may either enhance hepatic fibrosis and inflammation, or even inhibit fibrosis. Moreover, genetic background of orchestration apropos of leptin, hepatic dysfunction, metabolism and fibrosis in MASLD is mostly unclear. Therefore, the aim of this study was to analyze the associations of the ACE (I/D), PPAR-γ2 (Pro12Ala) genetic polymorphisms with hepatocytes' functional activity, leptin and fibrosis in patients with MASLD.

Methods: The study fully conforms to international bioethical standards and involved 96 patients (mean age 53.70 ± 5.34 years) with MASLD, 56 (58.33%) women and 40 (41.67%) men. Diagnosis and management according to EASL-EASD-EASO Clinical Practice Guidelines. The liver function was assessed by detoxification, protein-synthetic function of hepatocytes indices, by the presence/absence of cytolysis, mesenchymal inflammatory syndrome, or cholestasis. Liver fibrosis (F0–F4) assessed by calculating fibrosis scoring models, liver elastography, and liver biopsies performed in 62 patients. Leptin and adiponectin were measured in ELISA. Leptin resistance (LR) was calculated as the leptin/triglycerides ratio. PCR was used to study the CNPs of PPAR-γ2 (Pro12Ala, rs1801282) and ACE (I/D, rs4646994) genes.

Results: The distribution pattern of patients with different fibrosis stages was as follows: stage F0 – 22,58%; F1 – 19.35%; F2 – 27.42%; F3 – 16.13%; F4 – 14.52%. Liver protein synthesizing function did not suffer, regardless of the genes' SNPs. In ACE DD genotype, direct bilirubin, AST/ALT, were higher than in II/ID-genotypes. Conjugated bilirubin was higher by 22.24% and 20.55% ($p < 0.05$), AST – 2.12 and 1.71 times ($p < 0.05$); ALT – 1.32 times ($p < 0.05$);. Ala-allele carriers had higher rates of AST, ALT compared to Pro12-genotype of the PPAR-g2 gene – by 35.21%, 38.64%, and 29.81%, respectively ($p < 0.05$). The fasting glucose level was higher in all patients regardless of type 2 diabetes, requiring further clarification. Leptin is higher in women, regardless of MASLD type and obesity by 1.74–2.39 times ($p < 0.001$). In MASLD men, leptin was 25.39% higher than in men with MASH, $p < 0.05$. In case of 3rd degree obesity, leptin was higher than in 1 and 2 degrees, regardless of gender: in men by 48.99% ($p = 0.022$) and 43.55% ($p = 0.034$); in women by 53.34% ($p < 0.001$) and 50.98% ($p = 0.002$). Obesity was associated with high leptin content in men ($F = 77.95$, $p < 0.001$) and women ($F = 341.43$, $p < 0.001$), with LR increase ($F = 103.17$, $p < 0.001$) and decrease of adiponectin ($F = 44.84$, $p < 0.001$), and higher grades of fibrosis. In female D-allele carriers of the ACE gene, leptin exceeded the one in II-genotype by 22.19% ($p = 0.048$) and 28.73% ($p = 0.036$). In Pro12 genotype of the PPAR-γ2 gene, leptin exceeded that of the Ala-allele carriers regardless of sex: in men 1.99 ($p = 0.036$) and 3.75 times ($p = 0.008$), in women by 32.79% ($p = 0.015$) and 27.81% ($p = 0.043$). LR prevailed exclusively in male homozygous Pro-allele carriers, over Ala-allele carriers – 2.23 and 3.16 times ($p < 0.01$), in contrast to women, where such dependences were not found, despite higher initial level of both leptins itself and LR rate.

Discussion/Conclusion: Multiple factors including metabolic dysfunction, oxidative stress, and lipotoxicity have been confirmed to initiate inflammation and fibrosis in MASLD. Different studies demonstrated that leptin has an important role in promoting liver fibrosis, can be secreted not only by adipocytes, but also by activated stellate cells. Otherwise, leptin also has a protective effect on hepatic stellate cells apoptosis as TNFα-related apoptosis-inducing ligand can selectively target activated hepatic stellate cells for apoptosis, while leptin protects them activated from TNFα-related apoptosis. This study confirmed many previous findings and showed associations of adipocytokines activity, bilirubin, transaminases, fibrosis in MASLD with genetic polymorphisms.

29. Complex interplay of hepatic fibrosis, inflammation and immune response in experimental fast-food and methionine-choline-deficient diets

Ruslan Sydorchuk (Chernivtsi, UA), Andrii Sydorchuk (Neu-Ulm, DE), Bogdan Lytvyn (Chernivtsi, UA), Larysa Sydorchuk (Chernivtsi, UA), Mykhaylo Yarynych (Chernivtsi, UA), Iryna Sydorchuk (Siegen, DE), Igor Sydorchuk (Chernivtsi, UA), Petro Kyfiak (Chernivtsi, UA), Igor Plehutsa (Storozhynets, UA)

Introduction: Individuals with metabolic dysfunction associated liver disease (MASLD), particularly those with advanced hepatic fibrosis, are at an increased risk of liver-related events like gastroesophageal variceal bleeding, ascites, and cancer, often accompanied by cardiometabolic diseases, and have significantly higher overall mortality risk. A set of dietary and lifestyle related factors like obesity, metabolic syndrome, diabetes, insulin resistance are the main factors underlying MASLD, which becomes one of the most common liver conditions in civilized world. The expression of adipose tissue inflammation showed directly correlation with the MASLD severity and progression to MASH, cirrhosis, fibrosis and liver cancer. Consumption of higher caloric intake is increasingly emerging as a fuel of metabolic inflammation not only in obesity-related disorders but also liver fibrosis. Previous studies demonstrated that greater Mediterranean-style diet and Alternative Healthy Eating Index scores were associated with a lower risk of MASLD and fibrosis. However, studies designed to examine the relationship between dietary quality and hepatic fibrosis are limited. Therefore, we aimed to analyze possible associations of different diets with fibrosis, inflammation and immune response in MASLD.

Methods: Fifty adult Wistar-line rats underwent 20 weeks of either MCD diet (Methionine-Choline-Deficient Diet, containing high sucrose and fat without methionine and choline, essential for hepatic mitochondrial β-oxidation and for synthesis of VLDL), the classic dietary model for studying MASLD/MASH, or FFD (Fast-Food diet, containing high fat, high cholesterol, high fructose), which is another dietary tool for MASLD/MASH modelling. The study fully conforms to international bioethical standards and approved by respective institutional body. Another similar fifteen animals formed control, receiving standard chow diet with not more than 10–12% of calories from fat. Liver bioptates were a source for liver histology, fibrosis, and proinflammatory cytokines determination; fibrosis stage determined by the presence of pathological collagen staining scored as either absent (F0), observed within perisinusoidal/perivenular or periportal area (F1), within both perisinusoidal and periportal areas (F2), bridging fibrosis (F3) or advanced cirrhosis (F4). Hepatic collagen content, as a readout of liver fibrosis, was measuring by hydroxyproline contents via colorimetric assay, and quantified by calculating the collagen/area ratio, the area occupied by stained collagen relative to the total visual area of the microscopic sample.

Results: FFD fed animals developed mainly perisinusoidal/pericellular histological changes associated with mild to moderate F1 stage fibrosis, whereas MCD fed animals presented with paraacinar macrovesicular steatosis, severe inflammation,

hepatocellular ballooning, more advanced stage of fibrosis (mostly 2–3 stages), occurring in a perisinusoidal/pericellular, perivenular or bridging fibrosis patterns, associated with severe MASH. Quantification of liver fibrosis by measurement of collagen deposition in histological samples showed a profound increase in collagen deposition in both study groups (FFD – 3.2 and MCD – 3.7 times increase, $p < 0.01$ and $p < 0.001$, respectively). These findings were supported by contents of collagen in liver (6.8 and 7.5 times increase, $p < 0.01$ and $p < 0.001$, respectively). Both MCD and FFD diets significantly impacted body mass during the study period compared to control. FFD increased body mass by 95.36 ± 12.71% ($p < 0.01$), while MCD-related change was opposite – it even decreased body mass by 37.14 ± 11.09% ($p < 0.05$), supporting previous studies. Further changes in body mass were insignificant in both groups. FFD diet animals led to significant decrease of NK T-cells in liver bioptates compared to both control and MCD group ($0.01 < p < 0.05$), while difference between control and MCD group was insignificant ($p = 0.11$). IL-4 demonstrated no valid changes in the FFD fed animals ($p = 0.19$), but was significantly higher in MCD fed animals compared to control ($p < 0.01$).

Discussion/Conclusion: This study clearly supports existing associations of dietary habits and development of metabolism associated liver conditions. Inflammation and immune response play a key role in the pathogenesis of obesity-associated metabolic diseases, including MASLD/MASH. Studies on pathogenic and protective role of immune cells in MASLD and their relationship with fibrosis are controversial: it was shown that lack of NK T-cells may promote steatosis, inflammation, and liver fibrosis in high-fat or choline-deficient diets, whereas other studies showed NK T-cells play a role in promoting liver fibrogenesis and cirrhosis.

30. Discriminative value, associations and mediating effects of inflammatory markers for MASLD, at-risk MASH and increased liver stiffness in 11,072 U.S. individuals

Laurens Van Kleef (Rotterdam, NL), Ibrahim Ayada (Rotterdam, NL), Jesse Pustjens (Rotterdam, NL), Frank Tacke (Berlin, DE), Willem Pieter Brouwer (Rotterdam, NL)

Introduction: Inflammation is a key factor in the progression from metabolic dysfunction-associated steatotic liver disease (MASLD) to metabolic dysfunction-associated steatohepatitis (MASH) and subsequent fibrosis. We evaluated the discriminative value, associations, and potential mediating effects of 10 inflammatory parameters for MASLD, at-risk MASH, and increased liver stiffness measurement (LSM).

Methods: We included adult participants from NHANES 2017–2023, excluding participants aged ≥ 80 years or with excessive alcohol consumption, viral hepatitis, hs-CRP ≥ 50 mg/L or missing inflammatory data. MASLD was defined as CAP ≥ 275 dB/m with metabolic dysfunction, at-risk MASH as FibroScan AST (FAST) score ≥ 0.35, and elevated liver stiffness as LSM ≥ 8 kPa. The discriminative value was quantified by AUC analysis and DeLong test. Associations were assessed with

logistic regression. Mediation analysis examined the role of inflammation in the association between metabolic dysfunction and liver outcomes.

Results: We investigated 11,072 participants (age 49, SD: 17; 47% male), of whom 41% had MASLD, 6.5% at-risk MASH and 10.2% LSM ≥ 8 kPa. hs-CRP had the highest discriminative value for MASLD (AUC: 0.674) and increased LSM ≥ 8 kPa (AUC: 0.635) and ferritin for at-risk MASH (AUC: 0.697). Further analysis indicated strong and primarily non-linear associations for hs-CRP and ferritin with impaired liver health, e.g. the LSM ≥ 8 kPa risk for the highest hs-CRP quartile was 4 times higher than the lowest quartile (aOR = 3.94; 95% CI: 3.2–4.88). Finally, the highest levels of mediation were found for the association between abdominal obesity and at-risk MASH (24%; 95% CI: 18–33%) and LSM ≥ 8 kPa (30%; 95% CI: 24–37%).

Discussion/Conclusion: In a general population, inflammatory parameters, particularly hs-CRP and ferritin, show modest discriminative value but strong associations with impaired liver health and mediated in the association between metabolic dysfunction and impaired liver health. These findings underscore the potential of inflammation as a modifiable and easy measurable target in preventing MASLD and its progression into more advanced stages of liver disease.

31. Evaluating the diagnostic accuracy of non-invasive fibrosis scores against Metavir staging in chronic liver disease

Dusan Zaric (Belgrade, RS), Aleksandar Milic (Belgrade, RS), Dusica Vrinic-Kalem (Belgrade, RS), Dusan Zlatkovic (Belgrade, RS), Marijana Gacinovic (Belgrade, RS), Petar Svorcan (Belgrade, RS)

Introduction: Accurate staging of liver fibrosis is critical for managing chronic liver diseases. While liver biopsy remains the gold standard, non-invasive tests (NITs) offer practical alternatives. This study aimed to assess the correlation and diagnostic performance of APRI, FIB-4, FIB4+, and point shear wave elastography (pSWE) against METAVIR fibrosis staging in a single-center cohort.

Methods: We analyzed data from 50 patients who underwent liver biopsy and concurrent non-invasive fibrosis assessment. The METAVIR scoring system (F0–F4) was used as the reference. APRI, FIB-4, FIB4+, and pSWE values were compared using ROC curve analysis for significant fibrosis (≥ F2), advanced fibrosis (≥F3), and cirrhosis (F4). Optimal cutoff values were determined via Youden's index.

Results: Point shear wave elastography showed the highest diagnostic accuracy across all fibrosis stages. Estimated AUCs were 0.75 for ≥ F2, 0.88 for ≥ F3, and 0.90 for F4. FIB4+ demonstrated improved performance over APRI and FIB-4, particularly in advanced fibrosis (AUC 0.77 vs. 0.71 and 0.57, respectively). Projected optimal cutoffs for cirrhosis were: 9.62 kPa for pSWE (sensitivity 100%, specificity 84%), 1.37 for FIB-4 (75%, 68%), and 0.111 for FIB4+ (100%, 44%). APRI yielded lower diagnostic utility in all stages (AUC ≤ 0.57).

Discussion/Conclusion: In this single-center cohort, point shear wave elastog-

raphy demonstrated excellent performance in predicting liver fibrosis severity and outperformed serum-based scores. FIB4+ showed improved diagnostic value compared to standard FIB-4 and APRI, particularly for advanced fibrosis. These findings support the integration of pSWE and enhanced biomarkers such as FIB4+ into routine clinical practice for non-invasive fibrosis assessment.

32. In vivo CRISPR/Cas9 screens identify cell death inducing DFFA-like effector B as a therapeutic target of MASH

Xiaowei Zhong (Hannover, DE), Alexandra Bogomolova (Hannover, DE), Qi Peng (Hannover, DE), Vanessa Hamann (Hannover, DE), Sebastian Hook (Hannover, DE), Qinggong Yuan (Hannover, DE), Heike Bantel (Hannover, DE), Heiner Wedemeyer (Hannover, DE), Michael Ott (Hannover, DE), Asha Balakrishnan (Hannover, DE), Amar Deep Sharma (Hannover, DE)

Introduction: Metabolic dysfunction-associated steatotic liver disease (MASLD) and its progressive form, metabolic dysfunction-associated steatohepatitis (MASH), represent a growing global health burden with increasing incidence in both Western and developing countries. MASH is a major contributor to liver fibrosis, cirrhosis, and hepatocellular carcinoma, often progressing despite lifestyle interventions. While the recent FDA approval of Resmetirom marks a significant milestone, its efficacy in advanced stages remains limited. Therefore, there is an urgent need to identify novel, effective therapeutic targets capable of halting or reversing disease progression.

To identify and functionally validate novel therapeutic regulators of MASH using an unbiased, genome-wide in vivo CRISPR/Cas9 screening approach, with a focus on the gene Cell death-inducing DFFA-like effector B (CIDEB), and to evaluate its therapeutic potential via genetic modulation in mouse and human 3D liver models.

Methods: A genome-wide CRISPR/Cas9 screen was performed in mouse models of MASH under both prophylactic and therapeutic conditions using an mTKO sgRNA library. Hits were identified based on enrichment or depletion in hepatic cell populations. Among several identified candidates, CIDEB was prioritized for downstream validation.

CIDEB was inhibited using:

- AAV8-shRNA vectors for gene knockdown in vivo.
- Lipid nanoparticle (LNP)-delivered cytosine base editors targeting CIDEB in hepatocytes via mRNA transfection.

Therapeutic efficacy was assessed in two murine MASH models. In parallel, human liver bud models (3D co-cultures of PHHs, Kupffer cells, endothelial, and stellate cells) were established and subjected to MASH-inducing conditions (FFA + LPS + TGF-β), with CIDEB targeted via LNP-CBE delivery.

Liver tissues and organoids were evaluated for steatosis, inflammation, fibrosis, hepatocyte editing efficiency, and safety.

Results: The in vivo CRISPR screen identified 12 reproducible regulators of MASH, including known genes (e.g., Xbp1, Nr1i3, Dgat2) and novel candidates such as CIDEB. CIDEB expression was significantly downregulated in livers from MASH mouse models and human patients.

- CIDEB knockdown via AAV-shRNA and base-editing via LNP significantly attenuated liver steatosis, inflammation, and fibrosis in vivo.
- In healthy mice, hepatocyte editing efficiency reached ~72.9% without toxicity; in MASH models, editing was ~31.3% but remained therapeutically effective.
- In human 3D liver buds, CIDEB editing reached ~72.5%, leading to marked reductions in lipid accumulation, inflammatory cytokines, and activation of hepatic stellate cells.

Discussion/Conclusion: This study presents the first genome-wide in vivo CRISPR screen for MASH, revealing CIDEB as a critical regulator of disease progression. Targeted inhibition of CIDEB – via either AAV-delivered shRNA or LNP-mediated base editing – effectively ameliorated MASH phenotypes in both mouse models and human 3D liver constructs. These findings support further preclinical and translational development of CIDEB-targeting therapies as a novel treatment strategy for patients with MASH.

AUTHOR INDEX TO POSTER ABSTRACTS

(Name - Poster Number)

Registration via www.falkfoundation.org or simply scan and register.

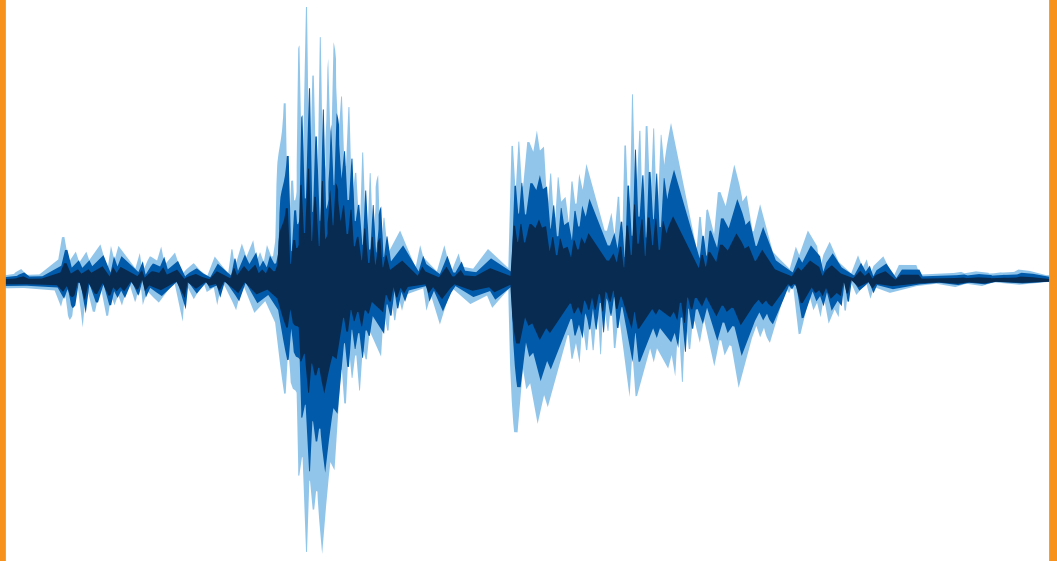

Together we know more. Together we do more.
Falk Foundation e.V. | Leinenweberstr. 5 | 79108 Freiburg | Germany
T: +49 761 1514-400 | F: +49 761 1514-460 | E-Mail: meeting@falkfoundation.org
www.falkfoundation.org